FACULTY OF INFORMATION TECHNOLOGY AND ELECTRICAL ENGINEERING

DEGREE PROGRAMME IN WIRELESS COMMUNICATIONS ENGINEERING

Measurements and Characterization of Optical Wireless Communications Through Biological Tissues

Author	Senjuti Halder
Supervisor	Marcos Katz
Second Examiner	Alexander Bykov

June 2020

Halder S. (2020) Measurements and Characterization of Optical Wireless Communications Through Biological Tissues. University of Oulu, Faculty of Information Technology and Electrical Engineering, Degree Programme in Wireless Communications Engineering. Master's Thesis, 63p.

ABSTRACT

Radio frequency (RF) has been predominantly utilized for wireless transmission of data across biological tissues. However, RF communications need to address several challenges like interference, safety, security, and privacy, which often hamper the communications through the tissues. To mitigate these challenges, light-based communication can be exploited, as optical wireless communications have unique advantages in terms of security, interference and safety. In this thesis work, we have utilized near-infrared (NIR) light to investigate the feasibility of optical wireless data transfer through biological tissues. To understand the basics of optical communications through biological tissues (OCBT), fresh meat samples and optical phantoms have been used as models of living biological tissues. An experimental testbed containing a data modulated light source and a photodetector was implemented to carry out different measurements regarding the OCBT concept. We have explored the influence of parameters like transmitted optical power, temperature of the tissue, tissue thickness, and position of the light source on the performance of the light-based through-tissue communication system. Analysis of the measurement data allowed us to compare and characterize the effect of used optical elements for better performance evaluation of the optical communication system. We have successfully transmitted a high-resolution image file through a 3 cm thick pork tissue sample. The maximum transmitted power through the tissue sample during the optical communication was 231.4 mW/cm^2, which is well below the limits defined by standard of safety regulation. A data rate of 22 kilobits per second has been achieved with the experimental system. Practical limitations of the current testbed prevented obtaining a higher data throughput. The results indicate a dependence of optical received power with respect to the tissue temperature. Moreover, we found both thickness and compositional differences of the biological tissues have a significant impact on the transmittance rate. This thesis work can be considered as a part of the development of 6G technology. The outcomes of this pilot study are very promising, and in the future, numerous potential applications based on OCBT could be developed, including wireless communications to implanted devices, in-body sensors, smart pills, and others.

Key words: Optical Wireless Communication, Near-Infrared Light, Biological Tissue, Implantable Medical Devices, Light Propagation, Optical Properties, 6G, Visible Light Communications.

TABLE OF CONTENTS

FOREWORD

The main objective of this thesis is to study the optical wireless communications through biological tissues using near-infrared (NIR) light. This Master's thesis has been conducted at the Centre for Wireless Communications (CWC), University of Oulu for the Degree Programme in Wireless Communications Engineering. This thesis work has been supported by Academy of Finland in 6Genesis Flagship Programme.

I would like to express my sincere gratitude to my principal supervisor, Prof. Marcos Katz for his immense support and guidance throughout the thesis work. Also, I extend my gratitude to Dr. Alexander Bykov for providing me with his valuable guidance as the second examiner of this thesis. I express my appreciation to Iqrar Ahmed, doctoral student of CWC for his useful feedback and ideas as a mentor which helped me understand the thesis objectives.

I also would like to thank Prof. Jari Iinatti for giving me the opportunity to join the research group of CWC. It has been a privilege to be associated with CWC and University of Oulu. I express my sincere appreciation to all my colleagues and friends from Networks and System research group at CWC for providing a cooperative and friendly work environment.

A heartfelt thanks go to my parents for their unconditional love, support, and encouragements which always inspire me to successfully accomplish the goals of my life. Finally, I would like to especially thank my husband Shuvashis for his tremendous support and guidance in every step of my life.

Oulu, 18 June 2020

Senjuti Halder

LIST OF ABBREVIATIONS AND SYMBOLS

IoT	Internet of Things
WBAN	Wireless Body Area Network
WPAN	Wireless Personal Area Network
HoF	Hospital of the Future
OWC	Optical Wireless Communications
IMD	Implantable Medical Device
MICS	Medical Implant Communications System
RF	Radio Frequency
BW	Bandwidth
NIR	Near-Infrared
LED	Light-Emitting Diode
LOS	Line-of-Sight
OCBT	Optical Communications through Biological Tissues
VLC	Visible Light Communication
DL	Downlink
UL	Uplink
IMDD	Intensity Modulation with Direct Detection
SCM	Single Carrier Modulation
OFDM	Orthogonal Frequency-Division Multiplexing
OOK	On-Off Keying
PWM	Pulse Width Modulation
M-PAM	M-ary Pulse Amplitude Modulation
M-PPM	M-ary Pulse Position Modulation
DFT OFDM	Discrete Fourier Transform-spread-Orthogonal Frequency Division Multiplexing
CAP	Carrierless Amplitude Phase Modulation
DCO OFDM	DC-Biased Optical Orthogonal Frequency Division Multiplexing
CSK	Colour Shift Keying
CIM	Colour Intensity Modulation
MM	Metameric Modulation
OW	Optical Wireless
PD	Photodetector
NLOS	Non-Line-Of-Sight
ITS	Intelligent Transportation System
V2V	Vehicle-To-Vehicle Communication
V2LC	Vehicular Visible Light Communications
DSRC	Dedicated Short-Range Communication
V2I	Vehicle-To-Infrastructure
HFR	High-Frame-Rate
GPS	Global Positioning System
RORWBAN	Reconfigurable Optical Radio Wireless Body Area Network
UDP	User Datagram Protocol
CNS	Central Nervous System
RTT	Radiative Transfer Theory
RWT	Random Walk Theory
MC	Monte Carlo

RTE	Radiative Transfer Equation
OOP	Object-Oriented Programming
GPU	Graphics Processing Units
CUDA	Compute Unified Device Architecture
OCT	Optical Coherence Tomography
CBS	Coherent Backscattering
DWS	Diffuse Wave Spectroscopy
IAD	Inverse Adding-Doubling
PDMS	Polydimethylsiloxane
NIRS	Near-Infrared Spectroscopy
PVCP	Polyvinyl Chloride-Plastisol
ZnO	Zinc Oxide
PVA	Polyvinyl Alcohol
PA	Photoacoustic Imaging
SOS	Speed of Sound
AA	Acoustic Attenuation
USRP	Universal Software Radio Peripheral
GMSK	Gaussian Minimum-Shift Keying
SDR	Software Defined Radio
LTE	Long Term Evolution
MIMO	Multiple-Input Multiple-Output
SIGINT	Signals Intelligence
DAC	Digital-To-Analog Converter
ADC	Analogue-To-Digital Converter
LO	Local Oscillator
ADE	Application Development Environment
SMA	SubMiniature Version A
AR	Anti-Reflective
PPM	Pulse-Position Modulation
PAM	Pulse-Amplitude Modulation
FSK	Frequency Shift Keying
MSK	Minimum Shift Keying
QPSK	Quadrature Phase Shift Keying
NEP	Noise Equivalent Power
PMT	Photomultiplier Tubes
ICT	Information Communication Technology
IoHB	Internet of Human Body

r_i	received set of symbols
H	channel response
s_i	transmitted set of symbols
ω_i	channel noise
I	intensity of transmitted light
I_0	intensity of incident light
μ_a	absorption coefficient
l	optical path length
l_a	absorption length
μ_s	scattering coefficient

l_s	scattering length
σ_s	scattering cross-section
C	volume density
g	anisotropy factor
$p(\Omega, \Omega')$	scattering phase function
N	number of scatterers
α	polarizability
λ	wavelength of light
R	distance from scatterer
θ	scattering angle
c	speed of light
D	photon diffusion coefficient
$S(r, t)$	source function
s	step size
ξ	random number
ΔW	absorbed photon weights
$\emptyset$	polar angle

1 INTRODUCTION

With the constant advancement of wireless communications technology, almost every aspect of our daily lives is getting greatly benefitted from its numerous applications. There has been a significant rise in adoption of the internet system globally and by the year 2023, nearly two-thirds of the global population are expected to have access to the internet. Thus, globally the number of internet users is projected to be increased from 304 million in the year 2000 to a staggering 5.3 billion in the year 2023 [1]. Simultaneously, there will be a rapid increase in the usage of mobile communication devices due to the on-going developments of the wireless technologies. These large numbers of devices as well as the increasing popularity of advanced large bandwidth-consuming services will result in several challenges like supporting high data rates and low latency, the need for secure and interference tolerant networks, etc. It is extremely essential for the new generation of wireless technologies to overcome the challenges.

In recent years, the Internet of Things (IoT), a future-forward technology appears to have a significant role in the enhancement of the wireless technology paradigm. IoT is considered as a state-of-the-art technology system with an aim to connect network devices and machines for exchanging information. Wireless communications have also made significant contributions to the betterment of healthcare. The medical industry is experiencing continuous developments due to the extensive use of various technologies such as wireless body area network (WBAN), wireless personal area network (WPAN), wearable devices, etc. Considering the rise of digital technologies, hospitals are in a state of major transformations in the future and the medical treatment would see a drastic improvement as well. The concept of hospital of the future (HoF) is primarily based on the purpose of having wireless connectivity among patients, health care professionals, medical devices. Due to their unique characteristics, optical wireless communications (OWC) have the potential to be exploited vastly towards future healthcare progress.

Moreover, there has been a growing interest in the advancement of 6G technology. The main aim of the Finnish initiative, 6Genesis Flagship program is the constant development and improvement of the research areas contributing to the 6G technology system [2]. There has been a significant enhancement in health care and living conditions over the past years and this enhancement makes smart health as one of the major focuses of 6G development [3]. In this thesis, optical wireless communications through biological tissues will be studied which is regarded as a part of the implementation of smart health. The future healthcare is expected to be highly benefitted by various usage of improved technologies. Light has a wide range of applications such as laser surgery, optical tomography, photodynamic therapy in the medical field developments as well as diagnosis and treatment of various diseases. Figure 1 presents a general overview regarding the basic concept of optical wireless communications where two scenarios have been considered. Firstly, an implantable medical device (IMD) is placed inside the human body and can relay information to the external device through an optical link. In the same way, it is also possible for an external device to be able to send information to the IMD. The other scenario can be considered as intra-body communication where the human body is regarded as the communication medium. Here, the communication takes place between two IMDs placed inside the body.

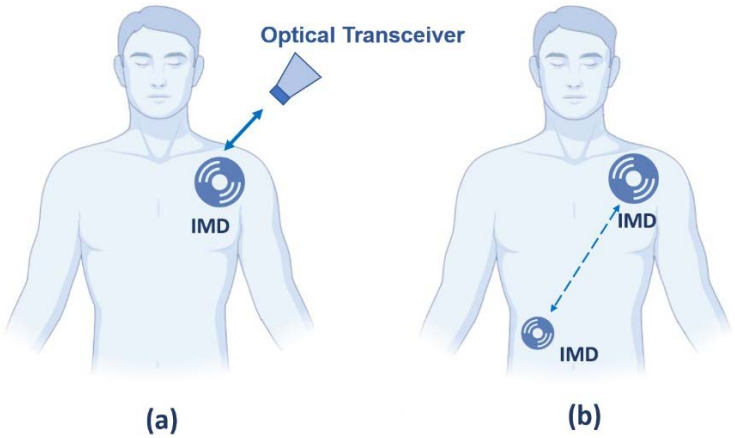

Figure 1. Schematic representation of (a) to and from IMD communication, (b) intra-body communication

1.1 Background and Motivation

In recent years, the utilization of information and communications technology in healthcare has been considerably increased due to its numerous advantages. The need for a better understanding of the body functions and constant physiological monitoring lead medical implants to play a significant role in the field of healthcare. Medical implants can either be implemented inside a human body or be placed on the surface of the body. Pacemakers, implantable cardioverter defibrillators, neurostimulators, medical delivery pumps are some of the examples of implantable medical devices [4]. Apart from transmitting the important body vital signs, IMD is also able to store delicate medical information. Wireless communications in healthcare as well as the medical implant communications system (MICS) are typically based on the existing radio technology.

Over the years, there has been a growing interest in exploiting optical wireless communications as an alternative to conventional radio frequency (RF) communications. Light rays have numerous applications in diagnostic and therapeutic medical applications. Although radio technology has been predominantly used for wireless connectivity, it still suffers from interference, security, spectrum congestion, issues regarding privacy, and safety. Moreover, IMD using the radio-based technology are more likely to get exposed to cyber-attacks due to the security issues of RF. According to some recent studies, there have been some staged attacks demonstrated to show the evidence that medical implants using RF technology are quite vulnerable to outside attacks which can severely breach the safety of patients' valuable medical data [5]. Any malfunction of the implants due to the deliberate attacks can result in serious health risks of the patient.

Optical wireless communications are undoubtedly capable of overcoming the drawbacks of radio communications because of its diverse advantages. Thus, both the wireless communications system can become complementary approaches to each other. The advantages such as increased security, larger bandwidth (BW), lower power consumption, non-interference, harmless for the human body, safety and privacy make optical communications a convenient approach for establishing communications through biological tissues. This thesis work is motivated to alleviate the various risks associated with RF regarding the wireless communications between the implanted devices and circuitry outside the body. Besides, the harmful impact on biological tissue as a result of RF radiation can be mitigated using optical

communications. It is challenging to remotely access optical communications link thus assuring the safety of both patients and important medical information.

1.2 Goal of the Work

A feasibility study of the optical wireless data transfer through biological tissues is presented in this thesis work. Optical communications can be viewed as a potentially safe approach for transmitting data through biological tissues. The main goal of this thesis is to establish successful communications through biological tissues using light rays. The reason behind utilizing light instead of conventional radio is to eliminate the drawbacks such as lack of safety and health risks associated with radio communications. Since this is a feasibility study, we would like to investigate the performance of biological tissue as an optical channel. In this work, we also aim to find initial results regarding how far inside the human body (eg., range) we can reach during the optical communications and the achievable data rate.

Here, for wirelessly transmitting data through biological tissue, near-infrared (NIR) of 810 nm wavelength has been used since NIR light has the best propagation characteristics in biological tissues. We have used biological tissue-mimicking phantoms and samples of fresh pork meat prepared for this purpose as the optical communications media. An experimental testbed has been used to carry out the measurements where the phantoms and biological tissue were illuminated by light-emitting diode (LED). On the receiving side, a photodetector has been used to detect the transmitted light ray which has a line-of-sight (LOS) communication from the LED.

Another aim of this work is to transmit a high-resolution image through both phantoms and meat samples. To analyse the feasibility of this optical communications, measurements of incident optical power, received optical power, and LED input current have been carried out. Characterization and comparison of the measured optical elements are conducted, and graphical relationships are presented to determine their effects on transmittance through the used samples.

1.3 Contribution of the Thesis

This thesis work presents a successful optical wireless communication through biological tissue using an experimental testbed. We have successfully transmitted data through a 3 cm thick pork meat sample using NIR light, allowing us to send a high-resolution image as well. Moreover, possible communications through phantoms mimicking human skin tissue illustrate the potential of optical communications through the complex structure of biological tissue. Comparison and characterization of the various optical elements prove the feasibility of optical communication through biological tissue (OCBT). This thesis also explains the effect of transmitted power, beam collimation, temperature of the tissue sample, thickness of tissue sample to better evaluate the performance of this optical communications system. It also discusses about the possible benefits of light being used for wireless communications through biological tissue.

1.4 Thesis Outline

This thesis consists of six chapters. The remaining of the thesis is organized as follows.

Chapter 2 consists of the necessary theoretical background and literature review needed to better understand the work of this thesis. This chapter contains five subsections that cover the concept of visible light communications (VLC). The first subsection provides a brief explanation of the properties and various important components of the VLC system. The next two subsections are focused on the advantages and applications of VLC, respectively. Also, some potential applications of both VLC and hybrid optical-radio wireless network systems are described in the last two subsections.

Chapter 3 focuses mainly on the optical properties of the biological tissues. This chapter consists of three subsections. The fundamentals of tissues and their classification are included in the first subsection. The second subsection covers the propagation of light through biological tissue, as well as some of the existing models for simulating photon transportation in tissues. Properties of the biological tissue-mimicking phantoms are described in the last subsection.

Chapter 4 is based on the implementation of the experimental testbed and the principles of the measurements taken for the experiment. It is divided into three subsections. In the first subsection, the experimental setup of the testbed is introduced, and the system model is described as well. A detailed description of the key components of the testbed is provided in the next subsection. Finally, the last subsection contains the measurement principles of the experiments regarding optical communications through biological tissues.

Chapter 5 presents and analyses the experimental results of the work that has been done in this thesis. Firstly, an elaborate description of the used tissues and phantoms is provided. The following two subsections present the measurement results and comparison among different scenarios considered for the experiments. Characterization of tissues and communication links are explained in the last subsection of this chapter.

Chapter 6 provides the overall summary of the thesis work. It provides a summary of the measurement results, system model, successful objectives of the research goals, and possible future research work.

2 BACKGROUND AND LITERATURE REVIEW

This chapter mainly focuses on the theoretical background that is needed to understand the thesis. This thesis is based on the concept of optical wireless communications through biological tissue. Near-infrared light will be used for wirelessly transmitting data through biological tissues. In this literature review, the basic concept of visible light communications will be described first. Then, the key components of VLC network such as transmitter, receiver, optical links, modulation schemes will be explained. After that, various properties and advantages of the VLC system will be covered. A brief comparison between radio frequency communications and visible light communications will be presented. It also illustrates the growing interest of VLC being utilized in the healthcare system. Finally, this chapter will cover the concept of the hybrid optical-radio wireless network system.

2.1 Visible Light Communications

In VLC, the visible spectrum is modulated for transmitting data. The visible spectrum extends over a wavelength of 400nm to 700 nm in the electromagnetic spectrum with frequencies between 430 THz and 750 THz [6]. Any transmission of data by modulating light waves in this range are part of VLC. The range of visible light spectrum in the electromagnetic spectrum is shown in Figure 2.

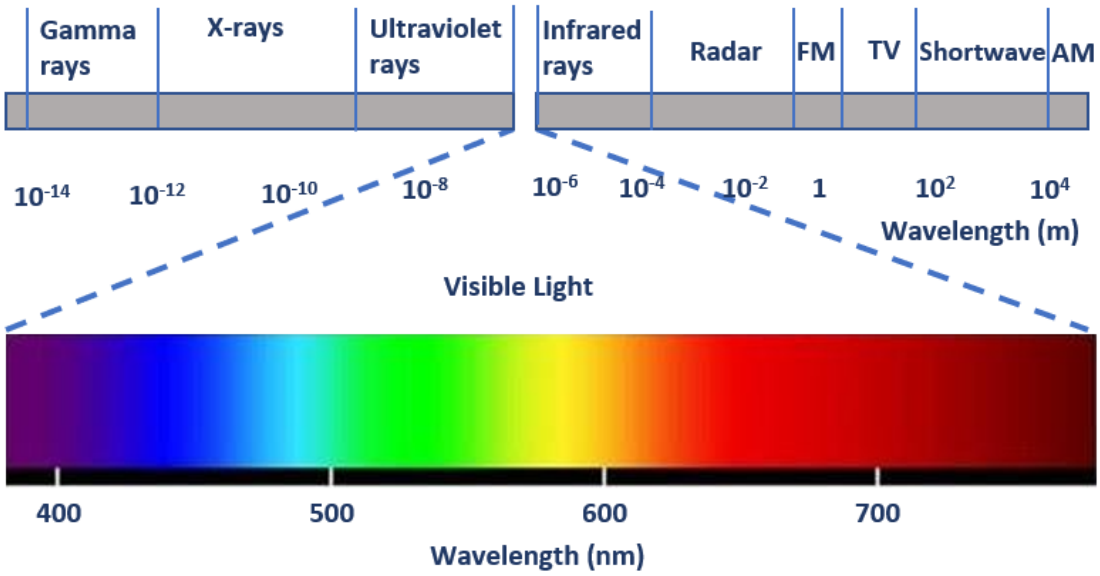

Figure 2. Range of visible light spectrum in the electromagnetic spectrum

Visible light communication is a fast-growing technology that uses fluorescent lamps or light-emitting diodes. In recent years, LED lights have become immensely popular because of their several advantages. They hold advantages like longer lifetime, energy efficiency, robustness, and good temporal stability [7]. Moreover, LEDs have the property of playing the role of both illumination and data transmission. This can be considered as one of the main reasons for LED to be used in VLC technology. The LED used in VLC can transmit data along with providing illuminance in a simultaneous way [8]. In this way, advantages like high data security, high bandwidth, larger data rate can be achieved during the communication [9]. Also, LED is the most energy-efficient as well as more durable among all the current lighting

technologies. The consumption of typical LEDs can be up to 65% less than conventional lamps. All these characteristics make LEDs as the most suitable choice for visible light communications [10].

A typical scenario of visible light communications is described in Figure 3. Here, it can be seen that, apart from illuminating the room, LED lights are also providing optical communication between various devices. Here, downlink (DL) is naturally carried out using the visible spectrum but uplink (UL) typically uses IR light, to separate the UL and DL channels and to avoid users being disturbed by light generated at devices nearby. It is possible to modulate LEDs at higher speeds. Since the modulation takes place at high speed, the human eye cannot see any blinking or fluctuation of the light intensity. Besides, they are not eminently directional and can be considered secure at high power while using in an indoor environment [11].

Figure 3. Schematic representation of an environment having VLC

VLC technology can be considered as a section of the typical set of optical wireless communications. Thus, VLC systems follow the same physical principles as optical communications. In the case of VLC, visible light rays play the role of a carrier which is also used for illumination. The main purpose of using VLC is to have communication and illumination simultaneously. So, it is always very important for VLC technology to have elements like transmitter and receiver. The visible light communications system can be divided typically into three parts, a transmitter, an optical channel, and a receiver. A block diagram of the VLC system consisting of these parts is shown in Figure 4 [12].

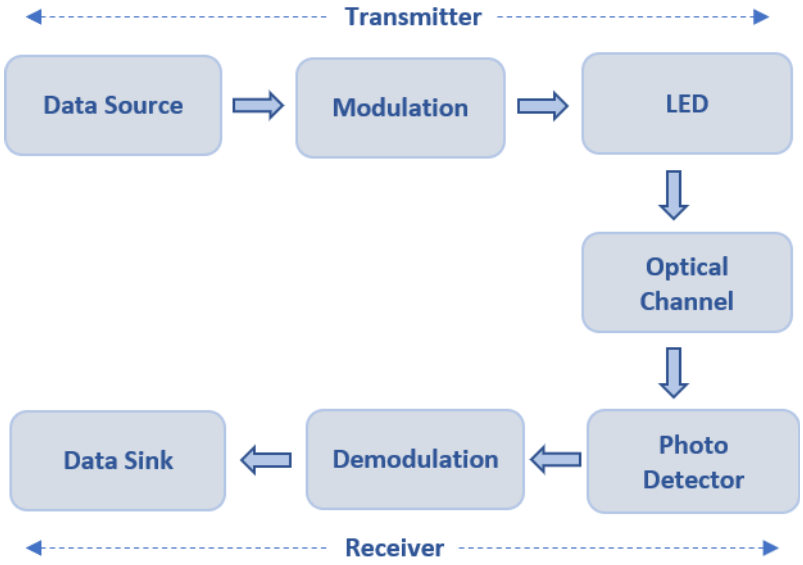

Figure 4. Block diagram of a VLC system

Intensity Modulation with Direct Detection (IMDD) is usually used in optical wireless communications. Over the recent years, various modulation techniques have been started to be associating with VLC. The modulation schemes compatible with VLC network include single carrier modulation (SCM), orthogonal frequency modulation (OFDM), colour modulation schemes. Again, these modulation schemes have some subdivisions which could well be used. SCM includes on-off keying (OOK), pulse width modulation (PWM), M-ary pulse amplitude modulation (M-PAM), M-ary pulse position modulation (M-PPM), DC biased OFDM (DFT OFDM) and carrier less amplitude modulation (CAP). There are several criteria regarding OFDM like DC biased OFDM (DCO OFDM), inherent unipolar, superposition OFDM, and hybrid. On the other hand, colour shift keying (CSK), colour intensity modulation (CIM), and metameric modulation (MM) can be included in colour modulation.

2.1.1 Transmitter

VLC transmitter part mainly consists of data module, modulator, and LED. The data can be sent by modulating the intensity of light by the LEDs. The transmitter of VLC plays the role of supplying the lighting of the place where it is situated. In general, any sort of lighting source can work as a transmitter device. The bulbs which are being conventionally used can have the capacity for several LEDs. The light needs to be modulated for the transmitted data modulation and there is a need for constant presence of light. Figure 5 represents a complete block diagram of a VLC transmitter. After the modulation of light, the channel's frequency response gets pre-compensated by the pre-equalization process. The illuminance of the bulb is controlled by a driver circuit which guides the course of current within the LEDs [13]. The transmission in visible light communication depends on contrasting the intensity of light where human eyes cannot spot the intensity fluctuations [14].

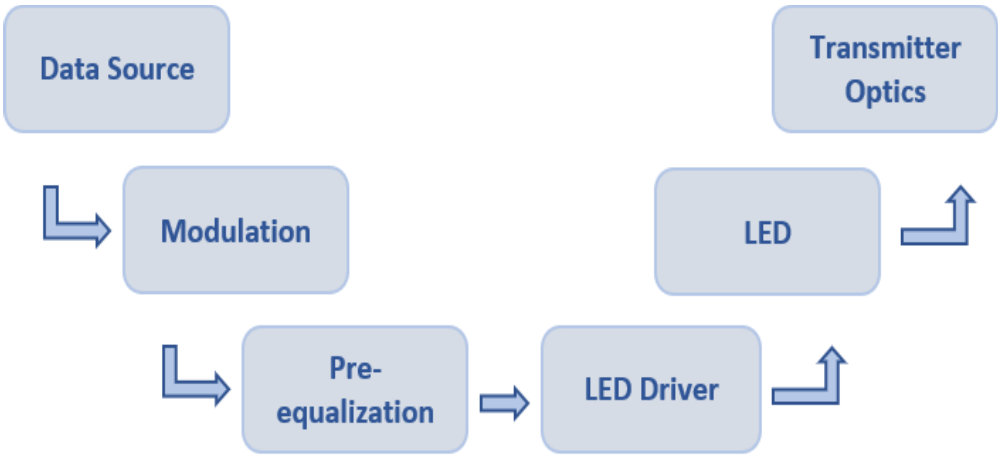

Figure 5. Block diagram of a VLC transmitter

2.1.2 Optical Channel

In general, the VLC channel is portrayed as the optical wireless (OW) channel. In VLC, LED light units are typically placed on the ceiling. In this system, LEDs work as the source in the DL transmitter. The optical communication channel is between the transmitter and the receiver. The channel's main purpose is to transmit the carrier signal. When the VLC is concerned, the channel happens to be the area between LED and photodetector (PD). In mathematics, it can be expressed with its transfer function, which is as follows [12],

$$r_i = H_{s_i} + \omega_i, \tag{1}$$

where, r_i is the received set of symbols, H is the channel response, s_i is the transmitted set of symbols and ω_i is the channel noise.

The VLC channels are grouped in a similar way like infrared links [15]. The configuration of links in both VLC and IR communications is quite identical to each other. The configuration varies due to the operating wavelength and devices like LED, photodetector which are dependent on the wavelength [16]. The dual characteristic of VLC (illumination and communication) also acts as one of the reasons for this variation.

VLC links can be classified into the following two approaches [15], and this classification is presented in Figure 6. The first criterion can be understood by the directionality of the transmitter and receiver. Based on this, there are three more subdivisions. The first one refers to the direction of the transmitter and the receiver towards a distinct point. This type of configuration is less prone to issues with artificial and ambient light sources. The next subdivision is where the transmitter and the receiver are not directed to a particular point and it is termed as a non-directional pattern. There are possibilities of larger optical loss and multipath-induced distortions with using this pattern. The power level would be elevated to overcome this situation. Also, there can be a variation between the directionality levels of transmitter and receiver [17]. This is referred to as a hybrid form and can be considered as the last of the mentioned subdivisions. In hybrid form, the transmitter is directed to a specific point but the receiver happens to be wide-field [18] and without being directed to a specific point.

The second criterion is classified on the basis of line-of-sight (LOS) between transmitter and receiver. Likewise, the first criterion, the second one is also classified into two subdivisions.

The first one belongs to LOS configurations, in which transmitter and receiver are in view of each other without having any obstacle between them. This system is power efficient and also makes the calculation of path loss less complex as reflection is not required to be taken into account. Non-line-of-sight (NLOS) configuration is the second subdivision in which the signal does not transmit directly between the transmitter and receiver as the path of propagation is obstructed (partially or completely) by obstacles [17]. The most convenient system would be the diffuse system consisting of NLOS configuration and a combination of non-directed transmitter and receiver. Summation of the LOS and diffuse components is applied to gather the channel bandwidth [19].

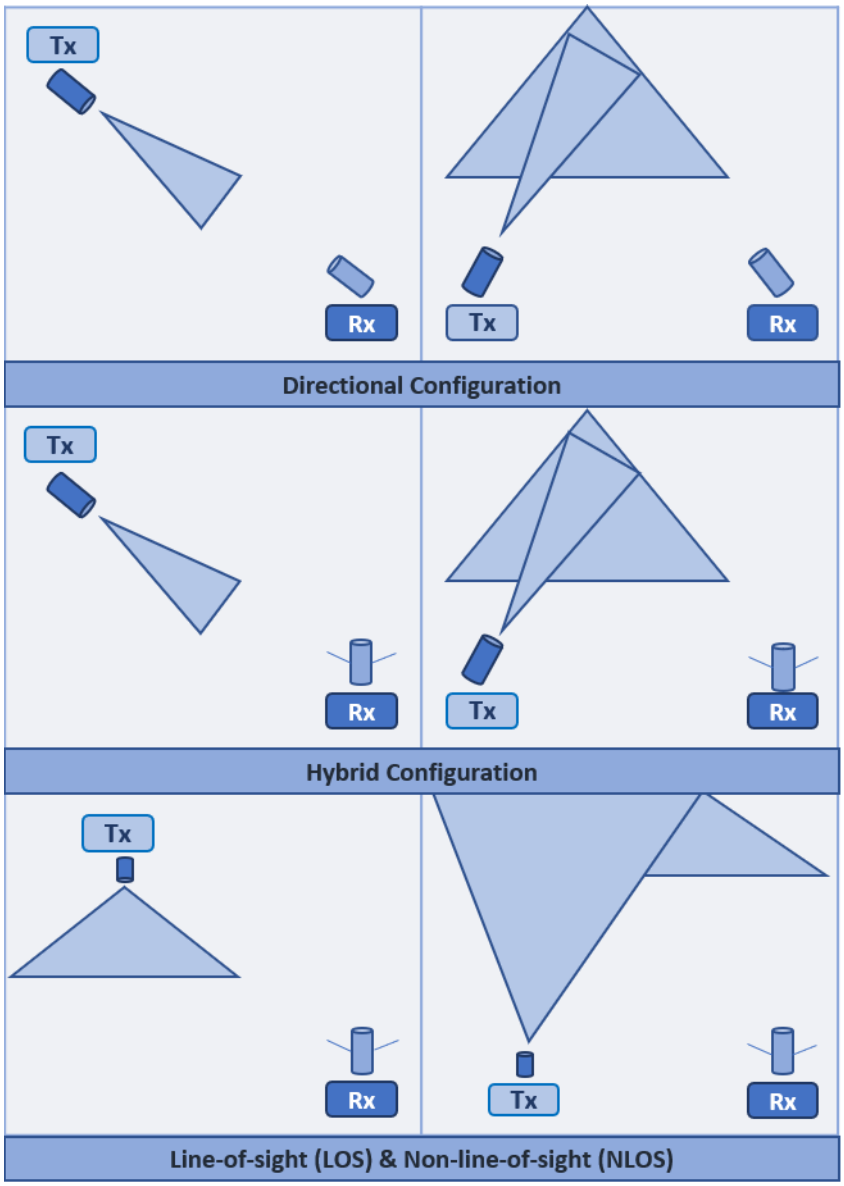

Figure 6. VLC link configurations [17]

2.1.3 Receiver

In the VLC receiver side, the photodetector is the principal component. Photodiodes and phototransistors are two major kinds of photodetectors [12]. A particular VLC receiver is

usually made of concentrator, optical filter, photodetector, amplifier, equalizer, and electrical filter. For receiving the VLC signal in a receiver, a photodiode is employed. Figure 7 shows a general receiver block of the VLC system. The purpose of the concentrator is to collect light signals going to the next component. The next component is the optical filter which works to tapering down the band. The filtered signal gets detected by the photodiode and transforms the optical signal into an electrical signal in a photocurrent format. A photodetector is one of the fundamental components of the VLC receiver. It is an electronic device which detects photon in order to generate electrons. The amplifier amplifies this photocurrent and for the enhancement of data rate, equalization is carried out [20]. The amplifier also helps to separate the desired optical signal from noise and interference [21]. As LEDs are usually on the ceiling, there would be at least one LOS signal on the receiver side.

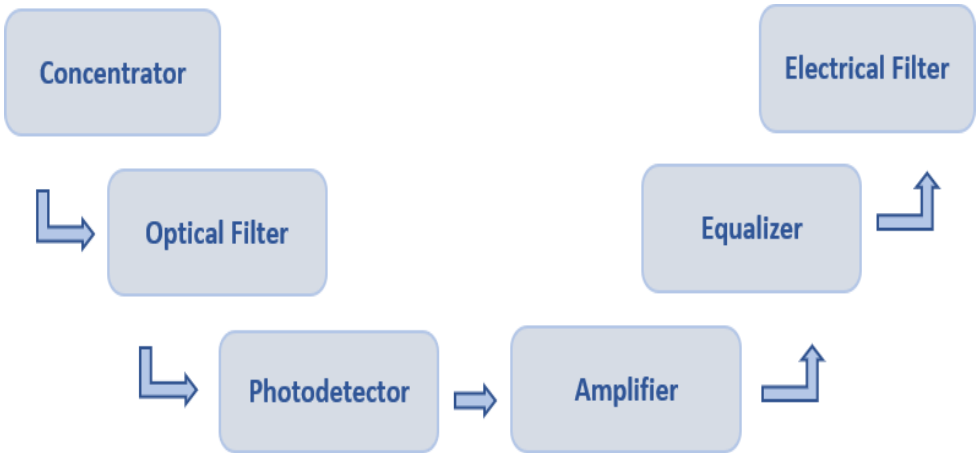

Figure 7. Block diagram of a VLC receiver

2.2 Advantages and Disadvantages of VLC

Visible light communications have been coming out as an interesting field of optical communication targeting the light spectrum visible to human eyes. Due to its availability and simple modulation with the use of LEDs, VLC holds several advantages. The main advantage of VLC can be considered as the ability of transmission of data and illumination simultaneously. Also, with the increase in usage of LED lights, VLC can be easily set up using the existing lighting infrastructure. Only by upgrading some of the existing lighting features, the whole communication system can be structured. Apart from this, there are many advantages to the VLC system which are mentioned below:

Efficiency: Light is modulated in VLC to transmit data. Typically LED lights are used for this system. In recent years, the usage of LED lights has been greatly increased. LEDs are regarded as significantly energy efficient when compared to other accessible lighting technology [22]. This energy-efficient property of LED makes visible light communications a green communications technology as well as environment-friendly [23].

Cost-effectiveness: LED lights have an extremely high lifespan ranging over e.g., 25000 hours of operation (at 70% lumen maintenance) [24], which means there is no need for frequent changing of the lights. For short-distance communications, VLC links can transmit at 4 Mb/s using optoelectronic devices costing only one US dollar per module [25]. Moreover, as visible light is used, the data transfer is almost free of cost. These superiorities can forge the overall VLC system to be cost-effective.

High-density coverage: Visible light communications can serve as reliable wireless access in certain places with a huge number of people. In those areas covered densely with users, the Wi-Fi system faces difficulties because of their spectrum limitations. Subsequently, every user tends to share the same access point spectrum. In VLC, all the LED bulbs light up a dedicated area which leads to creating small cells that provide coverage to a fixed number of people. In this way, there is no need for all the users to share the same access point, thus guiding to provide better network coverage [26]. Data speed of 15 Gbit/s can be achieved by VLC [27].

Bandwidth: Radio frequency refers to the rate of oscillation of electromagnetic radio waves in the range of 3 kHz to 300 GHz [28]. For communications transmission and broadcasting, this frequency band is typically used. On the other hand, VLC with a wavelength of 400nm to 780nm possesses 10,000 times greater spectrum availability than that of conventional radio waves [29]. It means VLC owns a significant amount of accessible bandwidth for data communication.

Safety: Visible light does not cause any risk to human health. Visible light assures the regulations regarding the safety of eyes, as the light is visible, high power is easily detected. Whereas, for IR light since it is not visible, high power is not detected and it could then be dangerous. So, following this regulation it can be used with optical power emitted to a larger degree compared to IR concerning the transmission distance [30]. The transceiver of VLC consumes less power as all signals in VLC transmission and reception end are at baseband and the optoelectronic component is responsible for the up-down conversion.

Interference: VLC usually does not cause any interference with RF signals [31]. This makes visible light communications a more suitable technology to be used in areas sensitive to electromagnetic waves.

Data security: VLC is regarded as a short-range communication system and is mostly suitable for indoor scenarios. Light does not penetrate through walls, also the spatial confinement of light beams make the communications intensely secure [32]. Moreover, light can be confined to a specific area and does not leave that area if any boundary comes up. So, visible light communication cannot be disturbed (e.g., jammed) by a third party. In contrast, radio waves can penetrate through walls and also eavesdrop is possible. In comparison with radio waves, VLC can be thought of as a more secure means of communication.

Spatial reuse: Visible light communications are operated by using light which is directional and encircled in a particular area. This phenomenon enables various non-interfering links to occur in neighbouring proximity [33]. In this way, bandwidth densities become high as well [34].

A summary of the comparison between radio and visible light communications is represented in Table 1.

Table 1. Comparison between radio and visible light communications

Property	Radio	VLC
Spectrum	30 Hz - 300 GHz	430 THz – 750 THz
Data rate	High	Very high
Safety for human	Less	High
Security	Low	High
Electromagnetic (EM) interference	Yes	No
Power efficiency	Medium	High
Range	Short-to-long	Short

Visible light communications are considered to be a very promising technology with numerous advantages and benefits. Although, it comes with a few disadvantages as well. One of the disadvantages occurs if at any point in time, unwittingly the receiver gets obstructed. As light cannot get over any objects other than transparent or translucent, the signal will be interrupted [35]. For VLC to operate optimally, two communication equipment need to have a direct line-of-sight. Although, NLOS operation is possible but, since the optical power falls significantly, the supported data rate could drop largely. Another issue of concern is the interference from different light sources both artificial and natural [36]. Additionally, as light is the base of the VLC system it can be a hindrance to use in places where darkness is required. Besides, VLC serves only as a short-range communication technology.

2.3 Applications of VLC

Features like free spectrum, data security, high data rate steer visible light communications technology to have a wide range of applications. It also has attributes such as larger bandwidth, immunity to electromagnetic interference, harmlessness to human bodies. All these traits have made VLC to be striking and appealing technology in recent times. Thus, there are plenty of scenarios and areas where VLC can be a suitable medium of communication. Some of the fields where VLC can be used effectively are stated below:

Indoor systems: The main prerequisite of establishing visible light communications is to have LED lights. Nowadays, most of the indoor places (homes, offices) are equipped with LED lights due to their various advantages over other commercially used lights. With the help of LED lights of the room, transmission of multimedia and television signal are possible [37]. The purpose of smart lights is to be able to remotely control the intensity and switching of implementing visible light communications in smart lights can provide illumination, control, and communications at the same time. Also, the energy consumption will be less, and the need for wiring would be limited as well.

Transportation and vehicle: There has been a rapid growth in using LED technology for vehicle lights, street lamps, traffic signals during recent years. Also, the front and rear lights of vehicles are implemented increasingly with the LED technology. A growing interest in intelligent transportation system (ITS) and increasing use of LED in automobiles lead VLC to be applied in vehicular communications. Visible light communications can be extended to a smart traffic system and in that way, different information (vehicle speed, traffic routes, etc) can be shared between the vehicles on road. This vehicle-to-vehicle communication (V2V) is of great use for preventing accidents and assuring safety on roads. The headlights of the cars can be considered as transmitters and inserted photodiodes can be considered as receivers [38] for the aforementioned communication. Due to the existing LED technology of traffic systems and automobiles, vehicular visible light communications (V2LC) is being regarded as simple and cost-efficient. Mostly the intelligent transportation system relies on dedicated short-range communication (DSRC) which is based on radio frequency, for instance, IEEE 802.11p. Positioning relying on VLC has some advantages over conventional DSRC as error rate in the former lies in tens of centimetres making it less prone to delays, packet collisions during the larger amount of vehicle on roads [39]. In [40] some more applications of VLC for vehicle-to-infrastructure (V2I) and V2V communication using image sensors have been proposed. Apart from the LOS attribute of the VLC system, here high-frame-rate (HFR) CMOS image sensors have been used, which can contribute to the safety of vehicular communications by image and video processing along with functions of VLC.

Underwater communication: Underwater communication is provided with many challenges compared to communications in air. An advanced and delicate system is needed to have successful underwater communications. RF communication cannot provide a satisfactory result when used underwater as the propagation is not efficient because radio waves get absorbed rapidly in water. Acoustic system is another alternative, but it has disadvantages like latency and low data rates. Water can only be transparent through visible band [41]; thus, visible light communications is suitable for underwater communications providing high-speed data rate over a short distance.

Mobile connectivity: Interconnection among smartphones, laptops, tablets, personal computers can be done using visible light communications in a similar way as Wi-Fi. Because of the short-range connection, it provides larger data rates and high data security.

Defense and security: Visible light communications can be implemented in military and defense services. These services very often deal with extremely sensitive data. As VLC technology is free from interferences it is not possible to alter the data from outside during communications. Besides having high communication rates, GPS-based systems can be substituted by positioning and range information in many places [42].

Location based-services: A potential application of visible light communications is in location-based services, where GPS receiver cannot work efficiently. For example, in an indoor place, a smartphone containing photodiode can work as a receiver. As the phone has photodiode, it can detect signals from the LED lights deployed in the room acting as the transmitter [43].

Indoor positioning system: VLC has great potential to be used for indoor positioning where short-range communications and low data rates are applicable. An application using this system could be very useful for the store owners as unexplored products can be made easily visible and at the same time, it can help the customers to easily find their desired products[44]. This system is highly beneficial for the customers as there is no requirement for any extra hardware to be attached in their respective mobile phones. Moreover, intensity modulation/direct detection and RF carrier allocation methods have been used for indoor positioning with VLC [45]. This process provides a high level of accuracy in positioning, where the error regarding the estimation of positioning is 2.4 cm.

Advertising industry: Plenty of billboards with different sizes and dimensions are seen on the roads used for advertisements. These billboards use a huge number of LED lights. Exterior network connection is achievable by utilizing the LED light intensity, which can be very beneficial to construct connections among users or traffics on road.

2.4 VLC in Medical Sector and Healthcare

Nowadays, hospitals are dealing with an increasing number of patients; as a result, doctors use wireless communications to track the situation of the patient in real-time to offer better quality care. Radio frequency technology is most commonly used in healthcare these days. Even though it is a very flexible and reliable medium of communications, but issues such as security and privacy, interference, radio exposure, and spectrum congestion make RF an unfavourable technology for certain scenarios in hospitals. Sensitive areas like operating rooms, around medical scanners RF communication is prohibited due to the impact of interference on delicate medical devices, health concerns of patients, the safety of medical records. However, these issues can be solved by using visible light communications in hospitals to lessen health risks. VLC being highly secure and free of interference can be regarded as a prospectively suitable medium of communications in future hospitals. In hospitals, VLC can greatly be applied to

monitor patients, networking, medical records storage, communication among various medical devices.

The usage of implantable devices for physiological monitoring has been increased in recent years. These devices are implanted by doctors and scientists to observe and study various properties of the human body [46]. Various important signals (e.g., electrocardiogram, glucose level, and blood pressure) can be relayed from implanted sensors to external equipment for analysis which can lead to both prevention and better treatment. So, it is crucial to have proper communication between the implanted devices and circuitry outside the body. Generally, wireless radio frequency telemetry has been used in several implantable medical devices. From various recent studies, it is known that the radio-based implanted medical devices are not utterly secure as sometimes they can be at risk of misuse [5]. There is a possibility of hacker attacks in heart devices using software or wireless communications leading to malfunctions which could be life-threatening at times. Implanted cardiac equipment may be susceptible to remote monitoring, which could lead to interruption, cyber security violations causing failures and drainage of batteries. Moreover, defibrillators that are implanted to prevent deaths from cardiac arrest are also vulnerable to hacking and could deliver unnecessary shocks to the heart or fail to respond. In a confined environment, optical signals transmit data in a more reliable manner because of the directivity and impermeability towards blockade. Also, a very significant small communication range makes light-based communications to be safe and secure.

VLC possesses no health hazards to the human body, and it can be used in association with various medical sensors. As light is an essential part of any hospital, the dual role of LED lights (transmission and illumination) makes VLC a promising technology to be used in hospitals. VLC can also serve as excellent guidance for the visually impaired people. In [43], the authors proposed a system using the LED lights as transmitter sharing location data and mobile phones as receivers. The mobile phone determines the ideal path and conveys the message to the visually impaired people using a headphone.

2.5 Hybrid Optical-Radio Wireless Networks

Conventional radio technology has been the most commonly used means of wireless connectivity over the years. Various advantages of radio technology including good propagation characteristics, existence of multiple standards, low cost, etc. have made it a predominant means of wireless communications. Despite being recognised widely, the radio-based system has some drawbacks such as sensitivity to interference, vulnerability to security attacks, radio exposure, spectrum unavailability, privacy, and safety. In recent times, visible light communications are being viewed to have the potential to be a revolution in future wireless networking. As discussed, VLC possesses several major advantages like larger bandwidth, interference immunity, energy efficiency, safe for the human body. All these advantages can be utilized to implement a hybrid optical-radio wireless network where radio and visible light-based communications complement each other. In this way, properties of VLC can neutralize the mentioned limitations of radio technology, thus provide a communication technology with better spectrum availability, energy efficiency, high data security. So, flexible and adaptive networking technology can be generated by using radio and light-based communications in a cooperative manner [47]. This hybrid network can satisfy the particular requirements of sensitive areas with the help of its flexibility and adaptability when the configuration is concerned.

The hybrid network, a combination of radio and light-based communication technology can be of great use in sensitive environments like hospitals. This hybrid technology has emerged

as an attractive area of research and several different concepts regarding the combined technology have been proposed. In [48] a hybrid VLC and RF point-to-point technology have been implemented, where the VLC link acts as the principal link, and depending on the availability it is considered to be an active link. If there occurs a cut off in the principal link, a vertical handover will take place between the nodes. The main focus of this hybrid technology is to create a combined system with an ability of handover between VLC and RF links. Another reconfigurable hybrid wireless network is described in [49], which is particularly suitable for future hospitals. Reconfigurable hybrid access points and reconfigurable optical radio wireless body area network (RORWBAN) are incorporated in the proposed network. Transmitter and receiver modes can be effectively adjusted by the network. Various operating modes of the hybrid transceiver is used in reconfigurable hybrid access points. In reconfigurable wireless body area networks, separate reconfiguration of network nodes is possible, and it works in the same way as general wireless body area network. The need for strict line-of-sight can often cause difficulties for proper communications using visible light, as light can easily be obstructed. For overcoming this problem, another hybrid optical-RF wireless network having fast network handover has been implemented. This system has the ability to rapidly switch over to the radio link whenever the VLC link faces any problem, e.g., light obstruction. Point-to-point user datagram protocol (UDP) data distribution was used while the rate of a dropped packet was taken as the performance measurement criterion [47]. In [50], another reconfigurable hybrid optical-radio wireless network system has been proposed. This network has the capability to be configured effectively according to the user's needs and operating conditions. Also, this hybrid network is considered to be a highly flexible and effective use of the resources is possible using the network.

Hybrid technologies would be very handy and convenient to implement in medical sectors. Some places in a hospital are sensitive to radio frequency. In those areas, hybrid networks can be viewed as the appropriate method of acting entirely as optical communications. Moreover, there might be a need for a larger bandwidth, in that case, data for transmission can be divided and transmitted through both radio and optical channel. The hybrid system also utilizes the property of high data security, one of the most important advantages of optical communications. Additionally, the link (radio or optical) with less power consumption can be chosen, making the hybrid system work as a low-power approach [49].

3 BIOLOGICAL TISSUES: BASIC DESCRIPTION AND PROPAGATION OF LIGHT

This chapter covers the basic description of biological tissues as well as the propagation of light through the tissues. Firstly, the fundamentals of tissue are discussed. Then, the principle of the propagation of light in biological tissues is explained. This chapter also discusses some of the existing models for simulating photon transportation in tissues. Finally, the chapter covers the description and properties of biological tissue-mimicking phantoms as well.

3.1 Fundamental of Tissues

The human body consists of trillions of cells which are viewed as the basic building block of the body. Cells are the functional and structural unit of any living beings and the structure of them depends solely on the cells. Cells have a complex structure with each part providing different functions. Apart from providing the structure of the body, some other important functions of the cells include generating energy from the nutrients of food, developing metabolic reactions, speeding up the growth using the mitosis process, helping in reproduction, etc. Cells having similar structure and function form a group which is known as tissue. Cells contributing to form a tissue come from a common origin.

The tissues of the human body are divided into four basic tissue types: epithelial tissue, connective tissue, muscle tissue, and nervous tissue. A brief description of these main tissue types is given in the sections below.

3.1.1 Epithelial Tissue

Epithelial tissues are considered as protective tissues that consist of a set of cells covering the external parts of the body as well as some surface of the internal organs. The outer layer of the skin, lining of the digestion tract, reproductive and urinary tracts are some examples of epithelial tissues. Depending on the number of layers of the cell and cells' shape, epithelial tissues are organized into different categories. There are three types of cell shapes such as squamous, cuboidal, and columnar. The shape of squamous cells is thin and compressed whereas cuboidal is squared shape with the same length and width. On the other hand, columnar cells are rectangular where length is higher than the width. Based on the number of cell layers, there can be three categories. The first one is a simple epithelium in which cells lie in a single layer and have direct contact with the basal lamina. The next one is the stratified epithelium that consists of multiple layers of cell and the basal lamina is connected only with cells with a basal layer. The last category is pseudostratified epithelium which consists of only one layer and the layer contains asymmetrical formation [51].

Epithelial tissues perform various functions in the human body. The cells covered under epithelial tissue are provided with mechanical strength and resistance by it. Their functions also include excretion, filtration, sensory reception, absorption, movement of substances. Moreover, they protect the internal organs from foreign agents, chemical stress, and radiation damage.

3.1.2 Connective Tissue

The connective tissue is the most diverse tissue that connects the other tissues to maintain the shape of organs. It contains extracellular matrix and provides structural and metabolic support for the tissues. Connective tissues perform various functions like protecting internal organs, helping with immune function, connection, and binding, storing, and transporting different nutrients. Connective tissues are classified into three broad categories such as connective tissue proper, supportive connected tissue, and fluid connective tissue. Depending on the composition, two types of tissues, loose connective tissue, and dense connective tissue are included in connective tissue proper. Apart from connecting tissues, it also provides shock absorption. On the other hand, in dense connective tissues, fibers are densely arranged and more resistance to stretching is provided [52]. Supportive connective tissues consist of bone and cartilage. They extend supportive structures for the other tissue types. Bones are the hardest connective tissue and act as supporting structures for the body by providing a rigid framework. They are comprised of cells, fibers, extracellular matrix, and help to store necessary components calcium and phosphorus. Cartilage is a firm connective tissue which is an important structural component of the body. It is made of cartilage cells and matrix. Matrix is a gel and contains cartilage cells and fibers. It helps with shock absorption to lessen friction, provides shape to nose and ear. There are three different types of cartilage found in the body, hyaline cartilage, elastic cartilage, and fibrocartilage. Blood and lymph are considered as fluid connective tissue. Blood contains a liquid ground substance called plasma and form elements like white and red blood cells, platelets. White blood cells protect from outside invasion while oxygen and carbon dioxide are transported by red blood cells. The lymph carries white blood cells and fat all over the body [51].

3.1.3 Muscle Tissue

Muscle tissues are composed of specific cells having the ability to contract when they get stimulated. This contraction leads to the generation of force and that allows the movement of bones. There are three types of muscle tissue in the body: skeletal, cardiac, and smooth muscle tissue [51]. Skeletal muscle tissue is made of long skeletal muscle fibers which are cylindrical. They are unseparated and placed in parallel with each other. Tendons bind some skeletal muscles to bones and these muscles control the voluntary skeletal movement. Skeletal muscle contains multiple nuclei and different striations. Cardiac muscle tissues also have one or two nuclei and striations. They contain intercalated discs and these discs help the cells of cardiac muscle tissue to be able to contract as a bunch. Cardiac muscles are found in the walls of the heart and they perform the process of pumping blood through the heart. The movement of these muscles is involuntary. Similarly, smooth muscle tissues also do not have voluntary control and the location of them are walls of some major organs and passageways. Their functions include transportation of various components like food, secretions through those major organs. The blood flow in arteries is controlled by them with the help of contraction [51].

3.1.4 Nervous Tissue

Nervous tissues are made of two types of cells: neuron and neuroglia. The nervous system carries signals from the brain to the rest of the body. Nervous tissues are located in the spinal cord, brain, and nerves.

Neurons consist of a cell body (soma), dendrites, and axon. The cell body has a nucleus and the nucleolus is surrounded by organelles. Dendrites are extended from the cell body and provide surface area for signal reception. The length of the axon starts from axon hillock and it has terminal branches at the end called a secretory region. Axon works as a conducting region and produces electrical impulses known as action potentials. Neurons can be categorized by functions and structures. Depending on the functions, there are three types of neuron: sensory, motor, and interneuron. Information signals get transmitted from sensory receptors towards the central nervous system (CNS) by sensory neurons, and motor neurons transmit signals from CNS towards muscles. Interneurons are very common in CNS and their purpose is to assist in the transportation of the information. Based on the structure there are three types of a neuron: unipolar, bipolar, and multipolar neuron.

The main function of neuroglia cells is to support and hold neurons in place. They are also classified into two categories: microglia and macroglia. Microglia provides the fundamental immune protection for CNS. Astrocytes, oligodendrocytes, Schwann cells are considered as macroglia. Functions of astrocytes include neuronal support, monitoring neuronal communication, damage repairing. Oligodendrocytes and Schwann cells protect neurons with myelin sheath in the central nervous system and peripheral nervous system respectively [51].

3.2 Propagation of Light in Biological Tissues

Biological tissues are considered as a turbid media and propagation of light through this turbid media is a quite complex phenomenon. For various biomedical diagnostics and therapeutic applications, it is extremely important to understand light propagation in tissues. Different biomedical applications vastly depend on the tissue optical properties. The optical properties of tissues are based on the fundamentals of light-matter interaction. Turbid media is heterogeneous and has strong scattering properties. The absorption coefficient, scattering coefficient, anisotropy factor, refractive index are the most important parameters for understanding the optical properties of tissue. Reflection and refraction need also to be considered when light propagation in tissue is concerned.

3.2.1 Absorption Coefficient

The absorption property of tissue and its various components (cells, cells organelles, etc.) act as a governing factor for the propagation of light in tissue. Hemoglobin, melanin, bilirubin, betacarotene are some of the main absorbers in the tissue [53]. The description of light propagation in absorbing medium (if the scattering is neglected) can be given with the Beer-Lambert law [54]. The value of absorption coefficient is measured from this so-called Beer-Lambert law.

$$I = I_0 \exp(-\mu_a . l), \tag{2}$$

where, I is the intensity of transmitted light I_0 is the intensity of incident light, μ_a is the absorption coefficient and l is the optical path length. A schematic representation of the transmittance rate is shown in Figure 8.

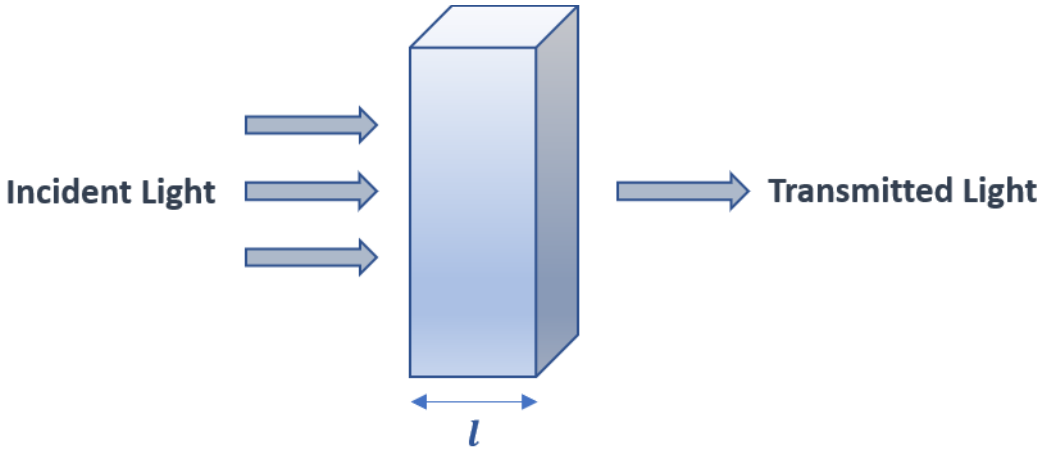

Figure 8. A schematic representation of the concept of transmittance

The distance in the medium until which a particular light ray penetrates through before absorption causes attenuation of the light beam is calculated from the absorption coefficient. The intensity of light gets dropped to e times after a specific length, known as absorption length. The absorption coefficient can be defined as,

$$\mu_a = \frac{1}{l_a}, \tag{3}$$

where, l_a is the absorption length and the unit of the absorption coefficient is mm^{-1}. All the optical methods rely on transmittance, reflectance, fluence rate, intensity [55]. For optical property measurements, *ex vivo* and *in vivo* methods can be used. In the *ex vivo* method, an experimental procedure is performed outside the living organism, whereas the experimental procedure is performed inside the living organism for the *in vivo* method. Measurements of absorbed light in both thick tissue and homogeneous large tissue are considered as *ex vivo* methods.

3.2.2 Scattering Coefficients

The mismatch of the refractive indices is the main reason behind the scattering of light in biological tissues. Heterogeneity of the biological tissue makes the scattering of light a difficult task. The distance in the medium until which a particular photon penetrates through before scattering causes attenuation of the light beam is calculated from the scattering coefficient. Scattering coefficients are determined by the average number of scattering events per unit length. The intensity of light gets dropped to e times after the scattering length. Scattering coefficient is expressed by [54],

$$\mu_s = \frac{1}{l_s}, \tag{4}$$

where, μ_s is defined as the scattering coefficient with a unit of mm^{-1} and l_s is the scattering length. Scattering in tissues is an important factor for both therapeutic and diagnostic biomedical applications. Scattering coefficients provide useful information about light dosimetry which is a key feature regarding therapeutic applications. Light wavelength and

different refractive indices determine the photon direction after scattering events. Light scattering can be caused by any compositional change of tissue components. So scattering properties are very helpful for the diagnosis of diseases. Scattering of light can occur either as elastic or inelastic type. Elastic and inelastic scattering refer to the change of the photon energy or wavelengths during the scattering. Scattering cross-section is a characteristic of the particle of the medium. The cross-sectional area of the scattering is defined as,

$$\sigma_s = \frac{\mu_s}{C}, \tag{5}$$

where, σ_s is the scattering cross-section and C is the volume density. The scattering phase function is a function of scattering angle, explains the distribution of intensity of scattering. The new direction of the propagating light after scattering is determined with the help of the phase function. In biological tissue, propagating light can scatter in various directions. Another essential characteristic of light propagation in biological tissue is the anisotropy factor expressed by g. This parameter is dimensionless, and it provides the direction of the scattering. Its value ranges from -1 to 1. Backward scattering is represented with the value of -1 and forward scattering is represented with a value of 1. The average anisotropy value of biological tissue is ~0.9. For visible wavelengths, the direction of light scattering in biological tissue is mostly in the forward direction and this makes biological tissue highly anisotropic. Anisotropy factor is considered to be the average of the cosine of phase function [56].

$$g = \langle cos\theta \rangle = \frac{\int p(\theta) cos\theta \, d\Omega}{\int p(\theta) \, d\Omega}, \tag{6}$$

where, $p(\theta)$ is the phase function. The attenuation coefficient of the tissue medium is the sum of absorption and scattering coefficients. It is expressed as μ_t,

$$\mu_t = \mu_a + \mu_s \, . \tag{7}$$

Due to the heterogeneous structures, biological tissues undergo Rayleigh and Mie scattering [54]. After a scattering event, the direction of light changes. This change of direction varies according to Rayleigh and Mie scattering. The size of the tissue particle determines whether the scattering would be of type Rayleigh or Mie. Rayleigh scattering occurs when the size of the particles is much smaller than the light wavelength. A strong dependency on light wavelength is present in Rayleigh scattering. Similarly, Mie scattering occurs when the size of the particles happens to be comparable to the wavelength of light. In Mie scattering, light scattering in a forward direction is more dominant and it is less dependent on the light wavelength, compared to the Rayleigh scattering [54][56][57]. Thus, after scattering, the light tends to propagate towards a generic direction. Rayleigh scattering equation is given by,

$$I = I_0 \, \frac{8\pi^4 N \alpha^2}{\lambda^4 R^2} \, (1 + cos^2\theta), \tag{8}$$

where, I is the intensity of transmitted light, I_0 is the intensity of incident light, N is the number of scatterers, α is the polarizability, λ is the wavelength of light, R is the distance from scatterer and θ represents the scattering angle. Figure 9 represents the Rayleigh and Mie scattering.

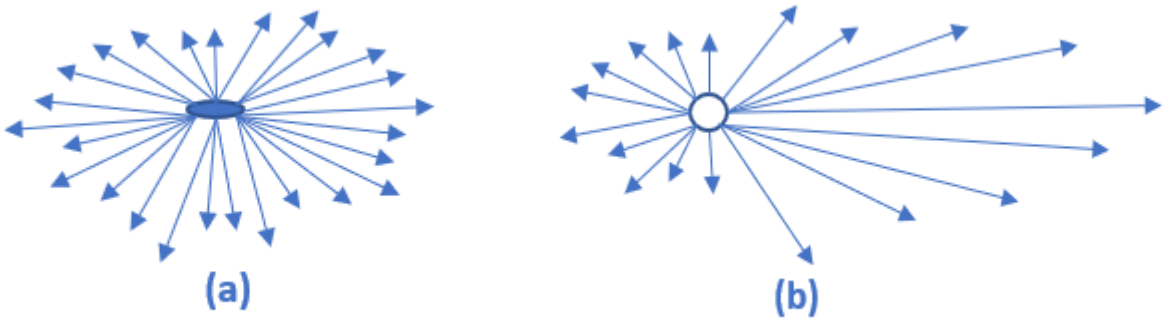

Figure 9. (a) Rayleigh scattering, (b) Mie scattering [58]

3.2.3 Reflection and Refraction

Biological tissues are made of multiple layers and this makes the light interaction with tissue quite complex. When light rays enter from one medium to another medium, depending on the refractive indices of the media and the incident angle, lights get reflected and/or refracted. The refractive index is an important parameter to effectively understand the interaction between light and tissue. Due to the multiple layers in a tissue structure, it is difficult to find the exact interface between different layers. Thus, determining the refractive index of tissue becomes challenging. Therefore, the average value needs to be taken from a specific tissue area for evaluating the refractive index. According to the fundamentals of light propagation, light propagating through a biological tissue should be reflected or refracted at the interface between two distinct tissue types. Since the heterogeneity of tissue formation, the reflection and refraction of light propagating through the tissue cannot be determined as a single phenomenon. Different internal tissue borders with different refractive indices are taken into account to evaluate various incidents of light reflection and refraction. These events are averaged to estimate the actual occurrence of reflection and refraction of light in biological tissue [54].

3.2.4 Existing Models to Describe Light Propagation in Biological Tissues

Photon transportation in a turbid media is a complex process and over the years several transport theory models have been developed to understand photon transportation. The methods can be classified as deterministic and stochastic methods. Electromagnetic theory and radiative transfer theory (RTT) (flux theory, adding-doubling method, diffusion approximation) are referred to as deterministic approach. On the other hand, the Monte Carlo method, random walk theory (RWT), photon path-integral formalism are considered as stochastic approaches.

The radiative transfer theory is an analytical approach to interpret the transportation of photons in tissues. Absorption, scattering in other directions cause the light intensity to be reduced. At the same time, scattering from other directions towards the initial direction increases the light intensity. In the RTT equation, this loss of intensity and increased intensity are added together to achieve the change in light intensity in a specific volume. The radiative transfer equation is given as,

$$\frac{1}{c}\frac{\partial I(\vec{r},\vec{\Omega},t)}{\partial t} + \vec{\Omega}\nabla . I(\vec{r},\vec{\Omega},t) + (\mu_s + \mu_a)I(\vec{r},\vec{\Omega},t) = \mu_s \int_{4\pi} I(\vec{r},\vec{\Omega},t)p(\vec{\Omega},\vec{\Omega}')d\vec{\Omega}' + Q(\vec{r},\vec{\Omega},t), \quad (9)$$

where, $I(\vec{r},\vec{\Omega},t)$ represents radiation intensity in direction Ω at point r, $p(\vec{\Omega},\vec{\Omega}')$ represents scattering phase function, c is the speed of light. Owing to the fact that biological tissue has multiple layers, light rays traveling through the tissue faces multiple scattering. These multiple scattering leads the photons to be diffused when it penetrates through a much deeper layer in tissue. This diffusion phenomenon can be explained by the diffusion equation,

$$\frac{1}{c}\frac{\partial \Phi(\vec{r},t)}{\partial t} - D\nabla\Phi(\vec{r},t) + \mu_a\Phi(\vec{r},t) = S(\vec{r},t), \quad (10)$$

$$\Phi(\vec{r},t) = \int I(\vec{r},\Omega,t)d\Omega, \quad (11)$$

where, D is the photon diffusion coefficient and $S(\vec{r},t)$ is the source function.

Monte Carlo (MC) is a very flexible and popular method for simulating photon transportation in tissues. Monte Carlo is a stochastic method and it provides a numerical simulation tool for photon propagation in biological tissue. This method is based on the expression of the direction of a photon using the radiative transfer equation (RTE) of photon transportation [59]. The probability distribution of the deflection angle due to the light scattering and photon transportation at the communication state of photon-tissue are used in this method.

Monte Carlo is a statistical method and it consists of some computational steps. Initially, a number of photons are transported through the tissue. When the photon is transmitted, it encounters various phenomena like scattering, reflection, refraction, absorption. After the photon is propagated, *s* defines the step size and *w* defines the weight of the photon [60]. The medium can be chosen as with either infinite or semi-infinite geometry. Step size is the propagation distance of photon within the location of interaction and it can be determined using the Beer-Lambert law and inverse distribution method. The step size, s can be written as,

$$s = -\frac{ln\xi}{\mu_a + \mu_s}, \quad (12)$$

where, ξ is considered as a random number, μ_a and μ_s are the absorption and scattering coefficients, respectively. After that, the movement of the photon gets started. The position of the photon is updated if it experiences any internal reflection after exiting the medium. In the case of no internal reflection, some parts of the photon weights are absorbed, and it can be defined by ΔW.

$$\Delta W = \left(\frac{\mu_a}{\mu_t}\right)W, \quad (13)$$

where, μ_t is the sum of absorption and scattering coefficients. The reflection and transmission of photons are also monitored during the computation. After the absorption, photons face the scattering process. Polar angle, scattering angle, anisotropy factor are the important parameters that need to be sampled and calculated during the scattering process. The scattering angle θ is often calculated using the Henyey-Greenstein function.

$$p(cos\theta) = 1 - \frac{g^2}{2}(1 + g^2 - 2gcos\theta)^{\frac{3}{2}}, \quad (14)$$

where, g is the anisotropy factor. The polar angle ∅ is defined as,

$$\emptyset = 2\pi\xi. \quad (15)$$

The absorption and scattering processes are continued until the photon leaves the tissue medium. The weight of the photon is compared to a threshold value so that the fate of the photon can be determined. If the weight is lower than the threshold, the Russian roulette method is applied [61]. This roulette technique is capable of deciding whether a photon with low weight will survive or not. After surviving the Roulette technique, if a photon is found to be the last one then the computation is considered to be finished. Otherwise, a new photon packet gets launched, and all the computational steps will be followed again.

Monte Carlo simulation can be employed for both homogeneous and inhomogeneous tissue models. The inhomogeneous model consists of multiple tissue layers. In the inhomogeneous case, it is possible that the photon can get hit between the existing layer and another layer of the tissue. Photon movement advances when it gets passed onto the next tissue layer or returns to the current layer. Moreover, a photon can also hit between the medium and the layer it is staying on. Calculation of transmittance and reflectance comes into play if the photon leaves the medium and it depends on the combination of the medium and tissue layers [62].

An object-oriented programming (OOP) based MC simulation model has also been developed which can enhance the simulation performance [63]. It makes the use of graphics processing units (GPU) and computes unified device architecture (CUDA) for the acceleration process. An online computational platform serving as a cloud-based Monte Carlo tool for photon transport is available for biophotonics applications [64]. The platform contains several applications to understand photon propagation. It can be a very useful tool for calculating sampling volume, polarization, skin spectrum, skin color, fluence rate, optical coherence tomography (OCT), pulse oximetry, coherent backscattering (CBS), diffuse wave spectroscopy (DWS), fluorescence, confocal microscopy.

3.3 Phantoms

Phantoms are the tissue-mimicking objects used for various biomedical experiments and diagnostics. The growing interest in utilizing optical techniques for biomedical applications has prompted the requirements of using these phantoms [65][66][67]. It is important to calibrate the devices for authenticating and validating the optical measurement techniques. Phantoms have properties like flexibility, less manufacturing time, durability, reproducibility, controlled optical properties, and phantoms that can be chosen based on these. The use of phantoms also limits the necessity of experimenting with real tissues as their optical properties might get degraded over time. The optical properties of the phantoms can be constructed according to their function. While mimicking a particular tissue, it is also important for a phantom to be able to perfectly replicate the tissue. Phantoms are very useful in examining the propagation of light in complicated multi-layered tissues [67].

Propagation of photons in tissues can be realized with the help of absorption, scattering, and scattering anisotropy. These factors need to be taken care of during the fabrication process of

tissue phantom so that they are perfectly similar to that of in tissues. Optical parameters like the absorption coefficient, anisotropy factors as well as the transmittance of the collimated light are needed to achieve the scattering coefficient [66]. For the successful fabrication of tissue phantoms, it is extremely important to match these mentioned parameters. Moreover, it is essential to choose correct materials while fabricating the phantoms in order to match the optical properties accurately. A number of different materials can be used for creating phantoms like titanium dioxide, aluminium oxide, polymer microspheres, zinc oxide, silicone, intralipid, albumin, agar, polyacrylamide gels, collagen, agarose, polyester resin, polyvinylchloride-plastisol, polyurethane, etc [68]. Among these, polyvinyl cryogels are heavily used in phantoms fabricated specially for medical applications. The optical properties of these phantoms can easily be modified, and this makes them a suitable choice for various applications such as optical elastography, biomedical optical methods, ultrasound, photoacoustic imaging, magnetic resonance imaging, diffuse optical imaging. Fibrin phantoms are fitted for experiments where organic materials are present.

Depending on the ways of obtaining light scattering, phantoms can be classified into two categories [65]. These are: nanoparticle or microparticle induced scattering and intrinsic scattering of the phantom materials. The first one is one of the most commonly used phantom types in which size, pattern, the concentration of the nanoparticle act as the deciding factors to obtain the proper light scattering. On the other hand, the other type does not contain any nano or microparticles and it has a homogeneous property with a relatively simple fabrication process.

A lot of different phantoms have been designed and developed to serve the purpose of biomedical optical experiments. The inverse adding-doubling (IAD) method is one of the most common methods for determining the optical properties of phantoms. Various techniques to measure the optical properties of homogeneous tissue phantoms mimicking skin are presented in [66]. Total reflectance, total transmittance, and collimated transmittance are very significant characteristics for understanding the phantom properties. These parameters can be measured with a spectrophotometer system with integrating spheres. Refractive index, dispersion characteristic, geometrical dimensions, surface roughness also play vital roles in calculating optical properties. The optical properties of the phantom can be then determined by using the IAD method in which the adding-doubling technique is used to interpret the radiative transport equation iteratively. Proper measurement of the phantom thickness is needed as the ground rule of this method lies on a sample of the infinitely thick plane-parallel slab.

Construction of phantoms with homogeneous property using an intrinsic scattering of the materials has been presented by the authors in [65]. They can be used in experiments where the bone and lung tissue need to be replicated. The inverse adding-doubling method following a spectrophotometric process is used here as well to attain the optical properties of the phantoms. These phantoms are made of two materials: a silicone elastomer polydimethylsiloxane (PDMS) and glycerol which is a transparent fluid. For these phantoms, instead of being used as a matrix material, a mixture of PDMS has been utilized as particle-free scattering material for the first time. The root of the intrinsic scattering was spotted by imaging the composition inside the phantoms by applying scanning electron microscopy. Quantity of glycerol has also been altered to see its effect on the optical properties. Glycerol does not react with PDMS as well as, polymerization of PDMS does not depend on the amount glycerol being used.

Phantoms are also made to mimic the multilayer tissue structure which are composed of a number of layers with various thickness. Capillary structures with vessels joined together having different widths can be placed inside these multilayer tissue phantoms [67]. Polyvinyl chloride-plastisol and titanium dioxide nanoparticles are used as materials for the phantoms.

Diffuse near-infrared spectroscopy (NIRS) is a popular method to examine different tissue parameters like oxygen saturation, oxygen in muscle, changes in blood volume, blood flow, etc. Phantoms with controlled optical properties can also be used for non-invasive optical diagnostic where different layers of the head including skull, skin, gray, and white matter [69]. These phantoms are a very suitable choice for experiments using the NIRS method. Polyvinyl chloride-plastisol (PVCP) zinc oxide (ZnO) nanoparticles are used as a matrix material and scattering material, respectively.

Stable, solid-state phantoms with controlled optical properties are needed for biomedical applications that involve the skin. Realistic vessel structure can also be incorporated in the phantom to mimic the pig ear skin [70] having exactly matched optical properties. Several different layers have been added to make a multi-layered complex skin phantom and the optical properties are evaluated by implementing Mie theory. Another useful method for estimating the important parameters of both tissue and phantoms like absorption coefficient, reduced scattering coefficient and anisotropy factor is Monte Carlo simulation.

Moreover, phantoms compatible for biomedical applications with laser radiation have been designed and developed by the authors in [71]. Treatment of skin lesions often requires laser therapy treatment. It is always a prerequisite for the devices to have tested for therapeutic efficiency. These preclinical experiments can be done using optical skin phantoms and applications of these phantoms are presented [72]. Phantoms constructed from polyvinyl alcohol (PVA) gel are popularly used in photoacoustic imaging (PA). For photoacoustic imaging methods, both optical and acoustic properties of the phantoms need to be tuned according to those of tissues. The spatial distribution of phantom parameters like the speed of sound (SOS), acoustic attenuation (AA), and reduced scattering coefficient have been analysed to study the compatibility of PVA breast phantom in photoacoustic imaging.

4 IMPLEMENTATION OF THE EXPERIMENTAL TESTBED

In this chapter, the experimental testbed will be introduced. At first, the OWC system implementation is described. The key components used for transmitting and receiving data have been explained. After that, different components and circuits used for the transmitter such as LED, LED driver, as well as the photodetector used for receiver, are described. The modulation scheme used for baseband carrier modulation is analysed. This chapter also discusses the measurement principles of optical communications.

4.1 System Description

An experimental testbed has been developed and implemented to examine, measure, and explore this particular through-the-tissue optical wireless communications. This testbed consists of mostly commercially existing products such as Universal Software Radio Peripheral (USRP), optical transmitter, optical receiver. In this work, the testbed is designed to create an optical wireless communication using NIR light. For this experiment, NIR light has been used owing to the fact that it has better capabilities to propagate through deep tissues. NIR light at a wavelength range of 650-1350 nm is considered to have the maximum penetration depth in tissues [73]. This improved penetration depth significantly makes NIR light a convenient choice. Biological tissues possess very strong absorption and scattering properties which makes the light propagation through tissues quite challenging. These absorption and scattering problems are less prominent by using NIR light. The testbed can provide great adaptability as the equipment used can be changed or connected with ease. The key components used in the testbed are the optical transmitter, optical receiver, and biological tissue. The system model of the VLC testbed is illustrated in Figure 10. The transmitter side consists of a computer, USRP, bias-tee, LED driver, and LED source. The components placed at the receiver side are photodetector, USRP, and computer. The transmitter and receiver for the system have been constructed with the help of USRP modules which are convenient and cost-efficient in terms of system designing. LEDs, LED driver, and detector are implemented with front end electronic components. GNU radio tunnel example has been executed using GNU radio software to build a tunnel between the source and receiving nodes. The GNU radio software has many modulation schemes to generate a baseband signal and we have selected Gaussian minimum-shift keying (GMSK) for this work.

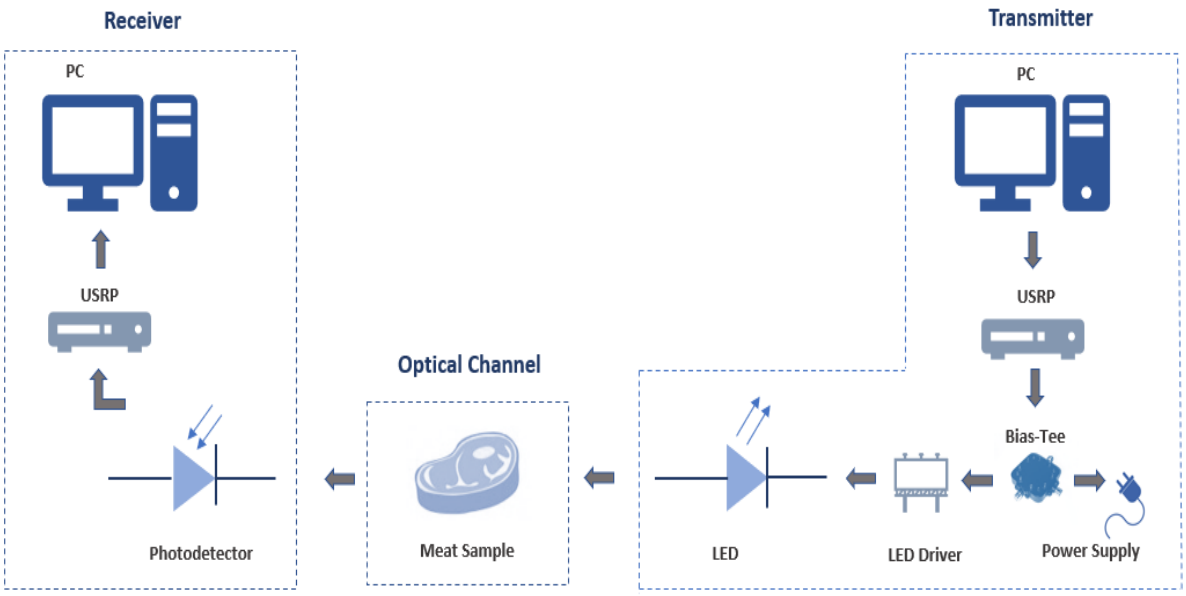

Figure 10. A system model of the optical wireless communications testbed

4.2 Description of Key Components of Testbed

In this section, different components of the OWC testbed have been described in detail. The separate explanation of the testbed components helps to completely understand the testbed. The specifications and functionality of the individual component are explained in detail here. At first, the optical transmitter portion is presented which contains a detailed description of the distinct components that the transmitter is consisted of. Then, all the components regarding the optical receiver are explained. A brief representation related to the chosen GMSK modulation scheme has been mentioned as well.

4.2.1 Universal Software Radio Peripheral (USRP)

USRPs are software-defined radio (SDR) devices developed and designed by Ettus Research, the daughter company of National Instruments. Instead of using hardware to carry out signal processing tasks, SDR technology utilizes software to establish RF communications. This technology allows a device to work with different standards after reconfiguration as the maximum universal unit of that device can be selected [74]. It is possible to design, implement, and prototype wireless communications systems by using USRPs which are typically transceivers having the ability to be reconfigured. These devices consist of a combination of host-based processors, FPGAs, and RF front ends. They can be of great use in cases of Long Term Evolution (LTE) testbeds, Multiple-Input Multiple-Output (MIMO) technologies, Wi-Fi testbeds, signals intelligence (SIGINT), radar systems [75].

For this work, two NI USRP-2920 with possible dynamic reconfiguration were used of which one is used for transmission and another one is used for the receiver. NI USRP-2920 has a bandwidth of 20 MHz and the frequency of the device ranges between 50 MHz to 2.2 GHz [75]. Both the USRPs are connected to the respective host computers by standard gigabit

Ethernet interface. LabView which works as an Application Development Environment (ADE) is installed in the computer and NI-USRP driver software is downloaded.

Communication between both transmitter and receiver USRPs is observed by configuring them accordingly. GNU radio is an open-source software toolkit equipped with various blocks for signal processing. GNU radio software provides tunnel examples through which a communication link can be established using USRP. A GNU radio tunnel example has been executed [48] [4] [50] and the associated program blocks work together to send data packets from one USRP to the other one. The transmission of data through these different blocks follows a particular procedure of linking the blocks. Network tunnel/network tap (TUN/TAP) driver from Linux is used by the tunnel example which acts as virtual network devices. Figure 11 shows the components that are associated with the tunnel software. TUN is regarded as a virtual device for the network layer, whereas TAP works as a virtual device for the data-link layer. A network interface is constructed by these virtual network devices TUN and TAP [47]. It is possible to obtain data packets of the network device from the user-space application. A virtual buffer is produced by the TUN driver thus allowing the data packets to be copied from user-space application to network device [48] [47]. Two virtual sublayers, MAC and PHY are included in the TUN network device. The transmitted data packets get processed and these sublayers are introduced. After processing, data packets are transferred from the source to the MAC sublayer. Then the packets get received by the PHY sublayer from the MAC sublayer and it forwards the data to USRP as the PHY sublayer is connected to the USRP [50].

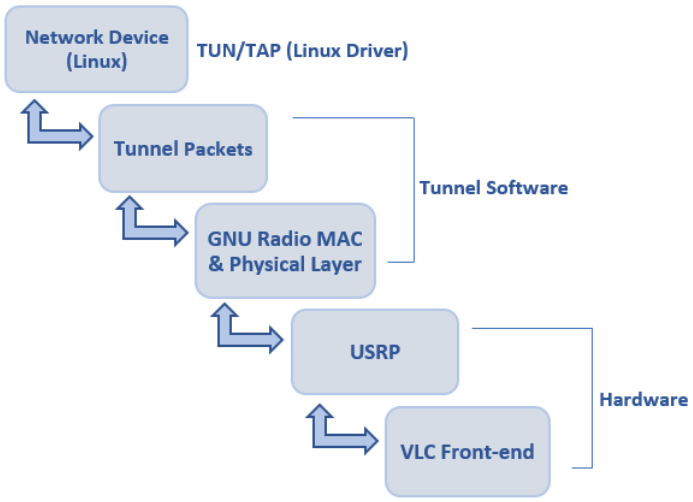

Figure 11. GNU tunnel software

4.2.2 Optical Transmitter

The purpose of the optical transmitter is to convert the information signal to be sent into light signals. An optical transmitter is comprised of elements namely data source, modulation, pre-equalization, LED driver, LED, transmitter optics. The working principle of an optical transmitter can be divided into two segments: the analog segment and the signal processing segment. The analog segment mainly contains the LED, LED driver, and transmitter optics. Data source, modulation, and pre-equalization are included in the signal processing segment. Sampling, modulation, and other necessary signal processing at the transmission side are handled by GNU radio, thus making the transmission setup quite simple and efficient [76] [77]. LED and LED driver might hamper the required linearity needed for the conversion of the

electrical signal to light [76]. Pre-equalization is responsible for correcting any occurrence of nonlinearity due to the LED or LED driver. The components of the analog part are described in the following sections.

4.2.2.1 Light Emitting Diode (LED)

In recent years, LED lights have become an essential part of the lighting technology due to their various advantages over other available light sources. This huge popularity of LED is mainly due to high energy efficiency, reliability, etc. LED can be considered to be the main component of VLC as it holds the attributes of providing lighting conditions and wireless communications simultaneously. LEDs are extremely energy efficient and high modulation bandwidth can be achieved by using them.

LED is a semiconductor diode in which visible light is emitted when an electrical current passes through it. This semiconductor diode is made of two semiconducting materials named p-type and n-type. A p-n junction is created from the combination of these two materials. A voltage is applied to this p-n junction where the positive side of the battery goes to the p-type portion and the negative side goes to the n-type portion, thus causing an electric field inside the p-n junction. In a p-n junction, the p side holds excess of 'holes' and n side hold an excess of 'electrons'. When the current flows through the junction, positive holes and negative electrons start moving in an alternate direction. The moment both holes and electrons recombine with each other, they release some energy in the form of photons.

For the developed testbed, an 810 nm mounted IR LED produced by Thorlabs has been used. This mounted LED includes a single LED that is mounted at the end of a heat sink. The wavelength of the used mounted LED is 810 nm and has 1 mm^2 of radiation spot. The heat sink at which the LED is mounted has a diameter of 30.5 mm. The output power of the LED is 325 mW and the bandwidth is 25 nm. A constant supply of current is needed for the operation of LED and the maximum supplied current should be 500mA. This current must be passed through at 3.6 V of forward voltage by the current source. The electrical power of the mounted LED is 1800 MW and it has a typical lifetime of more than 10000 hours. It has better thermal management property which allows the LED to have lesser optical power loss once it goes to the equilibrium temperature. To overcome any optical power loss decreased lifetime or overheating, it is extremely important to maintain proper air ventilation. The radiation emitted from LED is of high intensity, therefore direct staring at the IR light should be avoided [78]. During the experiment, protective glasses were used all the time to prevent any damage to the eyes.

4.2.2.2 LED Driver

A LED driver is an electrical circuit needed to control the LED. It drives the power that a LED has been given to. LED driver regulates the power provided to the LEDs. The input voltage of the LED can be converted to the required optimum voltage using a driver.

There are quite a few drivers that are compatible to be used with Thorlabs 810 nm mounted IR LED [78]. Among them, Thorlabs DC2200 LED driver has been used for this work [4]. This driver is mainly used for LED input current modulation. LED current of up to 10 A and a forward voltage of up to 50 V can be achieved from this LED driver. It can be controlled by using the front panel accompanied by a digital display. The back panel contains a SubMiniature version A (SMA) connector where the externally modulated voltage is applied, and the process

of modulating LED current is implemented. The LED current limit and the user terminal of the driver conversion/modulation coefficient are important factors regarding the conversion of the voltage to LED current. A wide range of internal and external modulations are supported by the DC2200 driver. One of the supported external modulation modes is Small Signal Bandwidth (Sine)[3] which can deal with the sine wave. The operating frequency for this Small Signal Bandwidth ranges between DC-250 kHz [79].

Another important component of this testbed is the DC bias-tee which is considered as one of the key elements of the testbed. The operating range of the DC bias-tee used in the experiment is 100 kHz to 4200 MHz at 0 V to 5 V. A bias-tee is a three-port electrical device that comprises a capacitor and an inductor. The purpose of using a bias-tee is to bias an RF circuit by supplying DC current or voltage. It works as a diplexer where the inductor blocks the AC signal allowing only DC signal to pass through. On the other hand, the capacitor blocks the DC bias and allows only the AC to go through. An equivalent circuit diagram of the bias-tee is shown in Figure 12. Here in the block (a), DC bias is added to the modulated RF signal already connected to one of the bias-tee ports from USRP. LED is provided with the required equivalent current by the driver, whereas the DC2200 driver is connected to the output of the bias-tee as shown in block (b). For illuminating the LED to the maximum, the DC bias has been set to 3.6 V, as LED has the capacity of having forward voltage of 0 V to 3.6 V. DC2200 driver can feed up to 400 mA of current to the LED for 1 volt applied. Thus, the LED input depends on the voltage that is applied to the bias-tee. The percentage of current coming from the LED driver can control the brightness of LED [4].

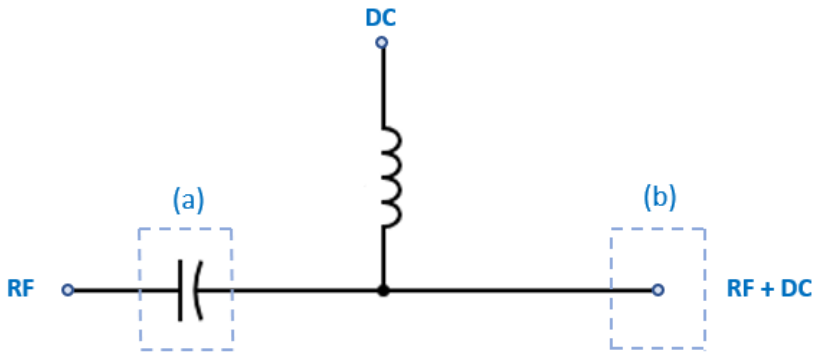

Figure 10. Circuit diagram of a bias-tee

A Thorlabs SM2F32B anti-reflective (AR) lens has been utilized to collimate the beam [4]. It helps to align the motion of the beam in a particular direction so that the amount of convergence or divergence gets reduced. The diameter of the adjustable collimation adapter is 2 inches with an operating range of 650 nm to 1050 nm and to mitigate the reflection it contains an anti-reflective coating [80].

4.2.3 Modulation Scheme

The selection of the modulation scheme for the OWC testbed plays an important role in the successful implementation of communications through biological tissue. Various factors like data rates, spectral efficiency, signal strength, a simple implementation need to be taken into account while choosing the modulation scheme. Pulse-position modulation (PPM), pulse-amplitude modulation (PAM), pulse-wide modulation (PWM), on-off keying (OOK) are some

of the schemes that are compatible to be used for visible light systems [76]. In this testbed, Gaussian minimum-shift keying (GMSK) modulation has been chosen and implemented.

Gaussian minimum-shift keying is considered to be a form of continuous phase frequency shift keying (FSK) modulation, where phase modulation and frequency modulation get incorporated. As a result, in GMSK there are no phase discontinuities and the spectrum is efficiently used. GMSK is viewed as a modified version of minimum shift keying (MSK) in which the phase gets changed in symbol intervals thus, a constant envelope is created. Here, the modulating signal directly changes the carrier signal phase. In GMSK, a Gaussian filter having a relevant bandwidth is deployed before the modulation part which is not present in the conventional MSK modulation scheme. A simple representation of the generation of GMSK modulation is shown in Figure 13. This pre-modulation Gaussian filter with sharp cut off and narrow bandwidth helps the output power spectrum to be used efficiently. Also, any unwanted deviation can be avoided using this filter as it possesses reduced overshoot impulse response [81]. This filter gives less out of band radiation and partial response MSK signals are created from the full response MSK signal [50]. This Gaussian low-pass filter curbs the RF bandwidth as well. At baseband, quadrature signal processing is employed with a quadrature modulator for the GMSK implementation.

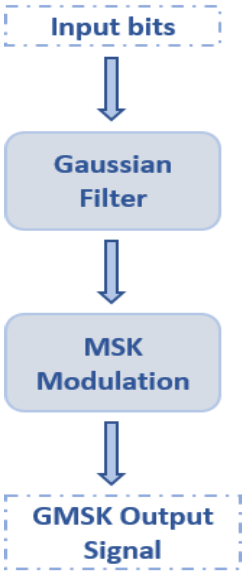

Figure 11. Generation of GMSK modulation

The transfer function of the low-pass filter used in GMSK is represented as [82],

$$H(f) = Aexp\left\{-\left(\frac{f}{B}\right)^2 \frac{ln2}{2}\right\}, \tag{2}$$

where, A is a constant, f is the frequency and B is the 3-dB bandwidth of the filter. Multiplying the 3-dB bandwidth and bit time, the time-bandwidth product is achieved. This product is an essential parameter for understanding GMSK modulation. To achieve more spectrum efficiency, it is important to have smaller BT products. However, for lower values of BT, inconsistencies of the GMSK signal from full-response MSK signal may occur. As this modulation scheme is provided with a constant envelope, the power efficiency of the scheme gets better. Some other advantages of GMSK include the capability of self-synchronization, higher spectrum efficiency, signal non-linearity, and lower power for the sideband.

The constant envelope property helps the GMSK to have an edge over the other conventional modulation schemes like quadrature phase-shift keying (QPSK), binary phase-shift keying (BPSK), etc. when it comes to optical communications. This is also the main reason behind choosing GMSK as the modulation scheme for this optical communications through tissues [4]. GNU radio provides inbuilt GMSK coding which makes the implementation simple and cost-efficient [76]. The instantaneous phase changes in QPSK modulation leads to signal deterioration as LED cannot cope up with that quick phase changes. The constant envelope of the GMSK provides steady phase changes thus, help to achieve better signal quality. Moreover, better bit-error-rate performance depends on the correct selection of the BT values in visible light communications [50].

4.2.4 Optical Receiver

The purpose of the optical receiver is to receive the transmitted optical signal with the help of photodetector and then convert the optical signal into an electrical signal. The optical receiver side can be divided into several individual parts. At first, photodetector detects the incoming light signal and this signal gets amplified. The amplification of the signal is essential for the signal to be demodulated correctly. The detected signal then goes through post equalization to further improve the signal for synchronization and demodulation.

4.2.4.1 Photodetector

In the optical receiver side, a silicon avalanche photodetector APD120A from Thorlabs has been used. The photodetector includes a silicon avalanche photodiode with high sensitivity and an ultra-low noise transimpedance amplifier. This high sensitivity is achieved using an internal gain procedure. The bandwidth range for this photodetector is from DC to 50 MHz. The wavelength range is 400 to 1000 nm and the maximum output voltage is 3.6 V for high Z load. The maximum input power is considered to be 1 mW and the CW saturation power is 1.5 µW. The effect of out-of-band noise can be mitigated by using an active low-pass filter that is included in an ultra-low noise amplifier. It is compatible to be used in cases where a low level of light detection is needed due to very less noise equivalent power (NEP). It can also be implemented instead of photomultiplier tubes (PMT). Transimpedance gain of the detector is 100 kV/A and with 50 Ω of termination, it becomes 50 kV/A. Any sort of outside ambient light can hamper the avalanche photodetector so necessary measures need to be taken when working with the photodetector. The diameter of the detector active area is 1 mm [83]. This diameter is not fixed and sticking an additional lens with the detector help to have a higher diameter. At 800 nm, the sensitivity of the detector reaches the highest point.

4.3 Measurement Principles

In this testbed, different materials have been used as the optical communications medium. The materials include optical phantoms and fresh meat samples prepared for this experiment. Measurements have been carried with different parameters, like transmission power, sample size, sample observation, beam collimation, etc. All the data obtained from the measurements have been characterized and compared.

Here, the used LED driver modulates the input current of LED, as mentioned in previous sections. The LED driver was excited with 3.6 V of externally modulated. The output power of LED has been monitored throughout so that the properties of biological tissue do not get altered. The biological tissue might get damaged because of the photothermal effect if it gets illuminated by LED for an excessive period. An exposure of 2 W/cm^2 of power obtained by 1 second of exposure at wavelength 830 nm is considered to be safe according to ANSI.Z136.1- 2007 [84]. In order to scale down the LED output power for the biological tissue safety, the modulating signal is varied.

Different sizes of meat samples have been used for the experiment. A sample piece of only pork meat as well as meat with some fat attached to it have also been used as an alternative to human tissues. In addition to the pork meat, biological tissue-mimicking phantoms with various thicknesses have been used for the experiments as well. Phantoms and different thicknesses of meat samples are placed individually between the LED and photodetector in an aligned position. A high-resolution picture was used as the information to be transmitted using all these optical communications media.

Meat samples having different thicknesses are taken to see whether the communications can happen through thicker slabs. The effect of tissue thicknesses on output power has been investigated. The transmittance rate of meat samples with different thicknesses has been obtained to better understand the penetration of light through the biological tissues.

A Thorlabs SM2F32-B adjustable collimation adapter with Ø2" lens with anti-reflective (AR) coating has been used to collimate the beam. This collimation adapter helps to narrow the beam of the light rays so that the rays become parallel and more aligned in a particular direction. Thus, the light rays experience less scattering when it propagates. The distance between the sample and surface of the lens has been varied to understand the effect of the used lens.

Additionally, measurements have been carried out both with and without the focusing lens to understand the effect of beam collimation. Measurements have been performed with both cold and heated meat samples. A heating box made of acrylic material has been used to heat the meat as well as to maintain the temperature constantly. A portable heater was placed inside the box and with the help of a temperature controller, the temperature was set to 37°C. Repeatability tests have been performed to evaluate the accuracy of the measurements. To understand the impact of the orientation of tissue structure, experiments are conducted by moving the placement of the tissue sample. The overview of the testbed for our measurement including all the components is presented in Figure 14.

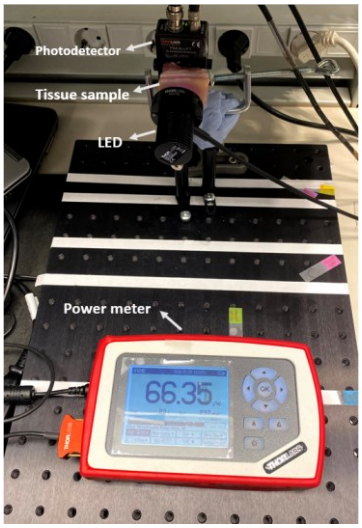

Figure 12. Overview of the experimental testbed

5 MEASUREMENTS AND CHARACTERIZATION

In this chapter, the measurement results will be analysed and compared. Firstly, a brief description of the used samples (fresh meat and phantoms) is provided. After that, the measurement data taken by varying different important parameters are presented and analysed. Finally, the results are compared and characterized in order to study the impact of the different parameters on the measurement results.

5.1 Description of Used Tissues

For this work, pork meat samples and optical phantoms have been used. The fresh pork meat, which typically possesses attributes quite similar to human tissue [85] has been taken from a local butcher shop. Here, three separate long pieces of pork belly meat with the skin on have been obtained from the butcher shop. The meat pieces have a quite homogeneous structure consisting of muscle and fat. These large belly meat pieces have been cut into different pieces according to the need of the experiments. Samples with four different thicknesses (1 cm, 2 cm, 2.5 cm, and 3 cm) have been taken for the measurements. At first, the measurements are carried out with meat samples at a cold temperature (11°C). Then the samples have been heated with the help of the heating box prepared for this work. The same experiments are repeated with the heated meat and the measurement data have been obtained.

The other sample used in this work is the biological tissue-mimicking phantoms that have been manufactured in the Optoelectronics and measurement techniques laboratory, University of Oulu [86]. These phantoms are fabricated to mimic human skin. The structure of the skin is complex and has multiple layers. Therefore, phantoms must be able to rightly replicate the skin's optical properties such as absorption coefficient, scattering coefficient, scattering anisotropy factor, refractive index, and thickness. The inverse adding-doubling (IAD) technique has been applied to determine these properties of the phantoms. The phantoms are made of polyvinyl chloride-plastisol and zinc oxide nanoparticles [69]. Five different samples of phantom have been used for the measurements. The samples presented in Figure 15 represent the scattering coefficients of 1 mm^{-1}, 2 mm^{-1}, 4 mm^{-1}, 6 mm^{-1}, and 10 mm^{-1} of skin thickness.

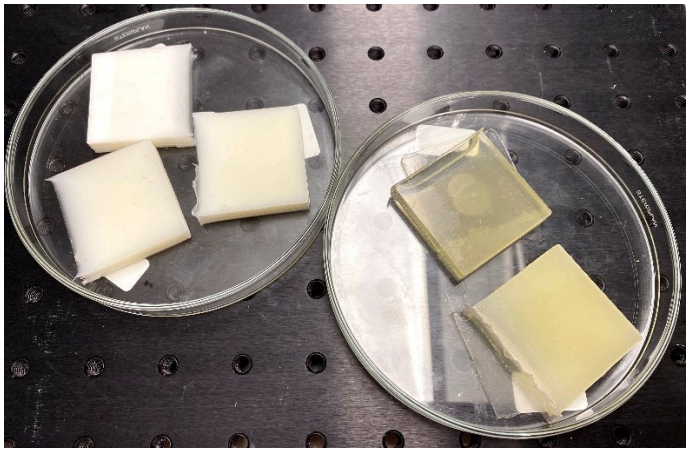

Figure 13. Skin mimicking phantoms used for the measurements

5.2 Results Analysis and Comparison

For the measurements, the Thorlabs NIR LED of 810 nm wavelength and the silicon avalanche photodetector have been placed in a LOS position. With the help of an LED driver, we modulated the input current of the LED. For the meat samples, two cases are considered for obtaining the measurement data. We have taken one set of measurements with the focusing lens attached to the LED. Another set of measurements has been done without the LED focusing lens.

First, we have tried to establish an optical communication through a 3 cm thick multi-layered meat piece (approximately 0.5 cm of fat and 2.5 cm of flesh). The temperature of the meat sample was 11°C at the time of this experiment. We have varied the LED input current, and respective optical power applied to the meat sample at these different levels have been measured. For both cases, we have been able to establish a successful optical communication through this 3 cm thick meat piece. Moreover, we have successfully transmitted a high-resolution image file of 14 MB through the 3 cm thick meat sample as well. Due to some practical limitations of the hardware used in our testbed including the prototype of the sample holder, we could achieve a date rate of some tens of Kbps. The transmitted optical powers to the 3 cm thick meat piece at different values of LED input current are presented in Table 2. From the table, it can be seen that the optical powers to the meat sample for these different input levels are well inside the safety limit as mentioned in the previous chapter.

Table 2. Optical power applied to meat sample

Input Current of LED (mA)	Optical Power to 3 cm Meat Sample (mW/cm^2)
100	50.94
200	101.11
300	146.26
400	190.53
500	231.38

The experimental setup of the optical communication through a 3 cm thick meat sample both with and without the use of focusing lens is presented in Figure 16.

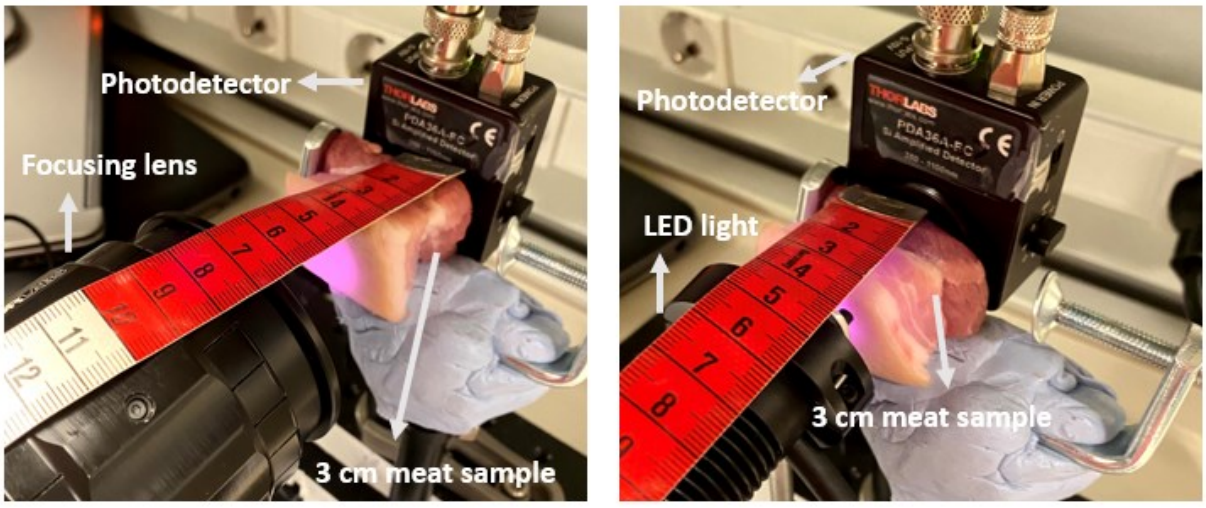

Figure 14. Experimental setup, (a) Optical communication using a focusing lens and (b) Optical communication without focusing lens

5.2.1 Impact of Beam Collimation

For the 3 cm meat sample, the received optical powers using a lens and without lens have been measured to investigate the impact of beam collimation. Figure 17 shows the amount of power transmitted through the 3 cm thick meat sample at varying input current of the LED. Two cases, with a collimated beam and without a collimated beam have been considered. The sample was placed 3.2 cm away from the lens as the focal length of our used lens is 3.2 cm. The LED without the lens was placed at 0.3 cm distance from the sample. Here, it can be seen the received optical power from the tissue sample varies significantly while comparing the two cases. When the light beam is collimated using the lens, it is observed that with the increase of per mA of LED input current, corresponding received optical power gets increased by 0.48 µW. On the other hand, without beam collimation, the received optical power increases by 0.93 µW with an increase of 1 mA input current. The overall received optical power appears to be relatively lower when we have used the lens. Due to some issues with our prototype sample holder, we could only use meat samples with a smaller surface area. The length and height of the meat surface facing the light were 4.5 cm and 3 cm respectively. So, this small area surfaces could not be able to properly fit all the parallel light beam that hit the surface. Similarly, the meat sample could not fully cover the photodetector sensor on the receiving side. This limitation regarding the size of the meat sample has resulted in signal losses. Additionally, although the lens used for beam collimation has anti-reflective coating still some of the light rays might get reflected from the surface of the lens.

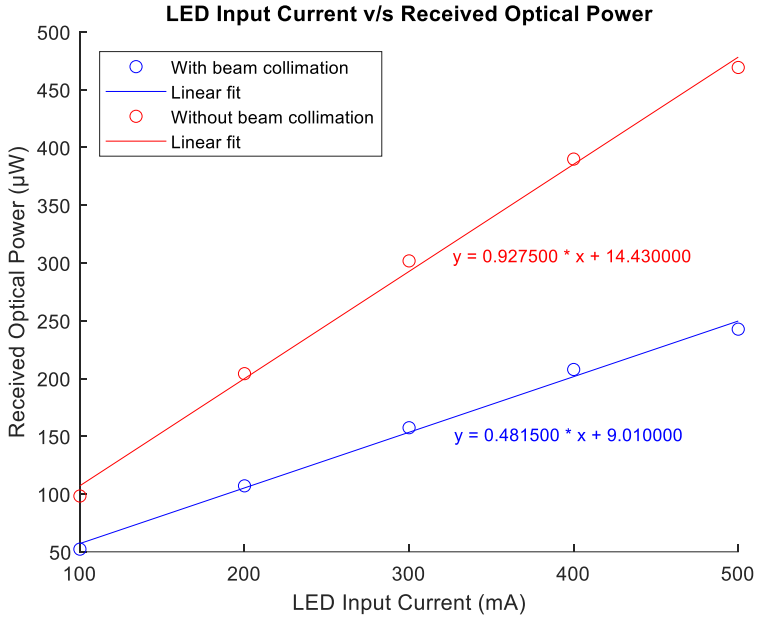

Figure 15. LED input current v/s received optical power for cold sample (11°C)

After that, we have heated the same meat sample to 37°C. The same experiment has been repeated for the heated sample as well. Figure 18 presents the amount of power transmitted through the 3 cm thick heated meat sample at varying input current of the LED. The optical communication was successful through the heated 3 cm thick meat sample as well. Here, we have also found that the use of focusing lens leads the received optical power to be significantly decreased. The slope of the fitted line indicates that, with the increase of per mA of LED input current the corresponding received powers increase by 0.49 µW and 0.95 µW respectively with and without beam collimation for the heated meat sample.

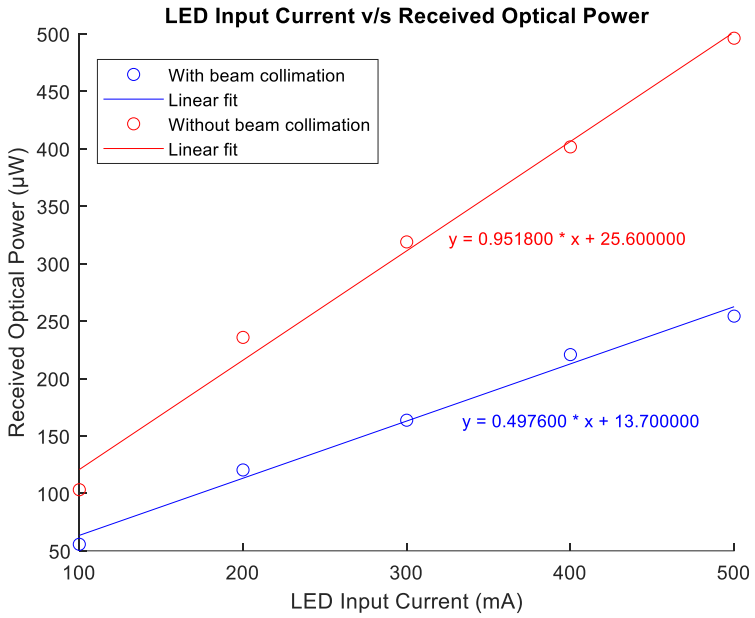

Figure 18. LED current v/s received power for heated sample (37°C)

5.2.2 Impact of the Tissue Temperature

When the 3 cm thick cold and heated meat samples were compared, we have seen a very slight difference in the respective received optical powers presented in Figure 19. From the slope of the fitted line, it can be seen the transmitted power through the heated sample increases by 0.95 µW with a per mA increase of the LED current. Whereas, the cold meat sample faces an increase of 0.93 µW, as mentioned previously. This variation in the received optical power is mainly due to the change of optical properties that occurs in the tissue when it gets heated. When the meat is heated to 37°C, the meat fat tends to become more transparent. This transparency of the fat causes a rise in the received optical power.

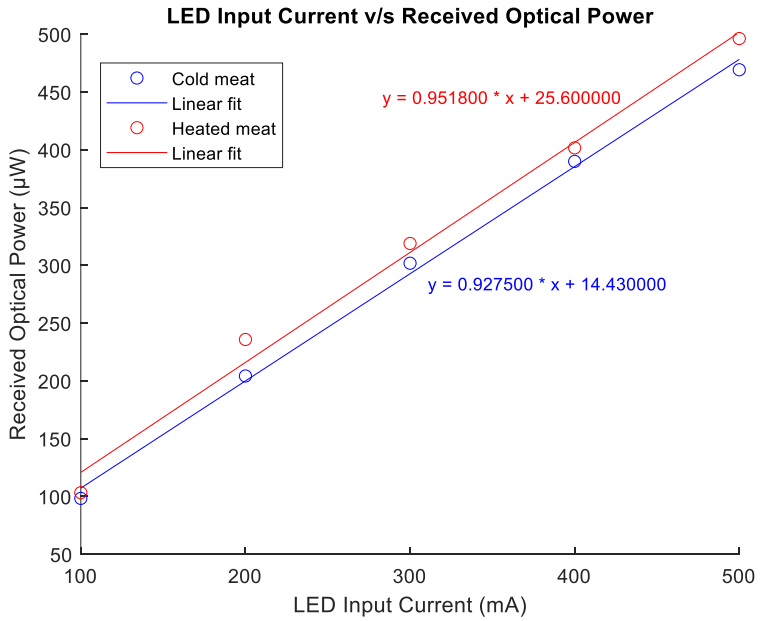

Figure 19. LED input current v/s received optical power for a cold and heated meat sample

5.2.3 Impact of Distance between Lens and Sample

In order to determine the impact of the beam collimation more precisely, the distance between the surface of the LED lens and the meat sample has been varied. We have placed the collimation adapter at twenty different positions for the experiment. The measurements of the received optical power corresponding to these twenty positions have been carried out. For these measurements, the input current of LED was set to 300 mA. Figure 20 shows the received optical power with respect to the distance between the LED lens surface and the meat sample. The plot indicates that the power transmitted through the tissue gets gradually decreased with the increase of the distance between lens surface and sample. The maximum received optical power has been detected at a distance of 0.5 cm.

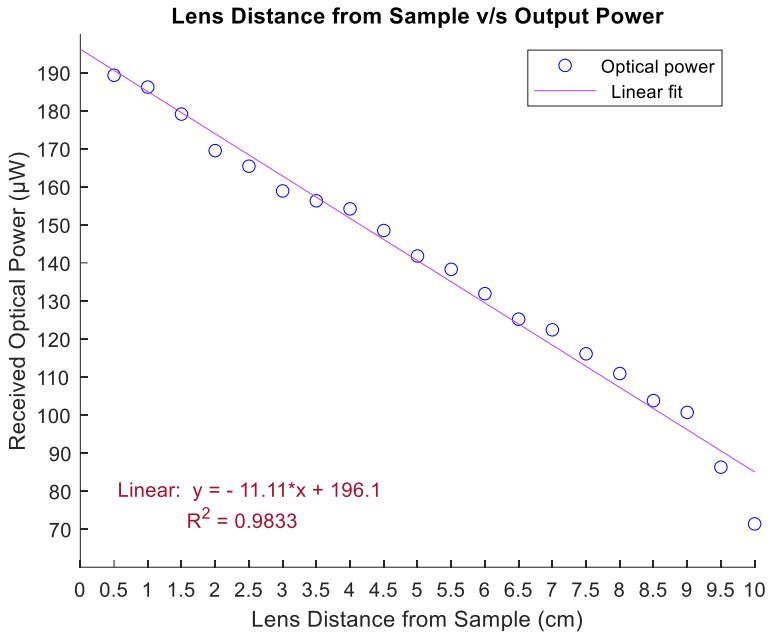

Figure 16. Effect of lens distance from the sample on output power

5.2.4 Repeatability Tests

In order to check the accuracy of our measurements, an inter-sample repeatability test using a 3 cm thick meat sample has been performed. It is highly required to conduct the same experiment multiple times with the same sample following the same conditions every time. We have obtained the received optical power of this sample six times keeping all the experiment procedures, measurement criteria, optical parameters unchanged. The input current of LED was set to 300 mA during these six observations. Figure 21 represents the variation in the output power of a 3 cm meat sample for six different observations. It is noticed that the received optical power with respect to the number of observations suffers from a minor variation. However, this variation can be considered negligible as the obtained *p*-value is 0.713. So, it could therefore be said that the measurements being carried out have a good accuracy rate.

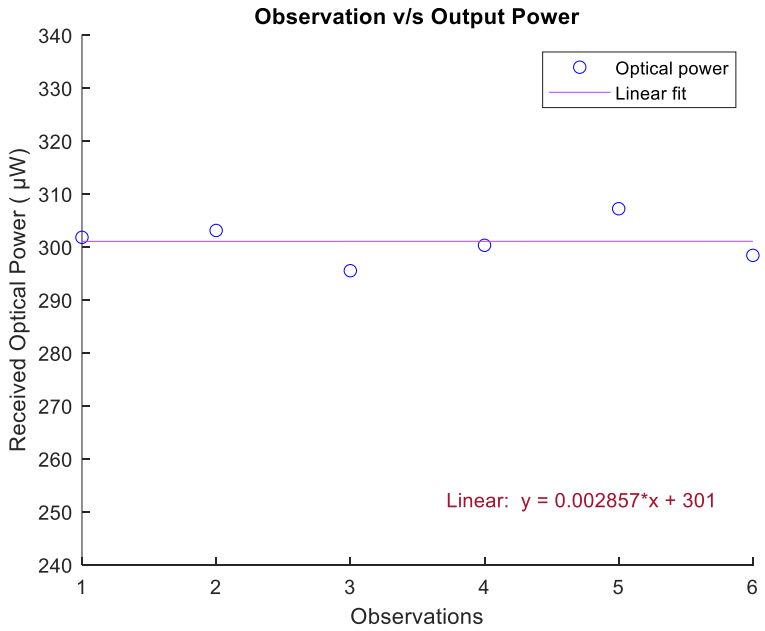

Figure 17. Output power variation for six individual observations

Another experiment has been conducted by using six different meat samples all having a thickness of 3 cm. All these meat samples belong to the same pig and represent the complex multi-layered structure of biological tissues. These six meat samples taken for this experiment are shown in Figure 22. Among these, five samples have been taken from five different positions of three separate belly meat chunks. The sixth sample has been taken from the front forearm of the pig. All the samples except from sample number 5 which belongs to the forearm, consist of multiple layers of fat and flesh. Sample number one consists of 1.5 cm of fat in multiple layers and a total of 1.5 cm of flesh. Similarly, sample number 2 is made of 1.3 cm fat and 1.7 cm of flesh. Sample number 3 has a very thin layer of fat compared to the rest of the belly meat samples. The thicknesses of the fat and flesh are 0.8 cm and 2.2 cm, respectively. The total thickness of the fat in sample number 4 is 1.9 cm along with a 1.1 cm of flesh. However, the tissue structure of this particular sample is quite complex. Sample number 5 that belongs to the forearm area has a relatively dense layer of flesh with a thickness of 2.8 cm and 0.2 cm of the fat layer. Whereas, the sample number 6 has a fairly similar structure with 1.4 cm fat and 1.6 cm flesh, compared to that of the sample number 1.

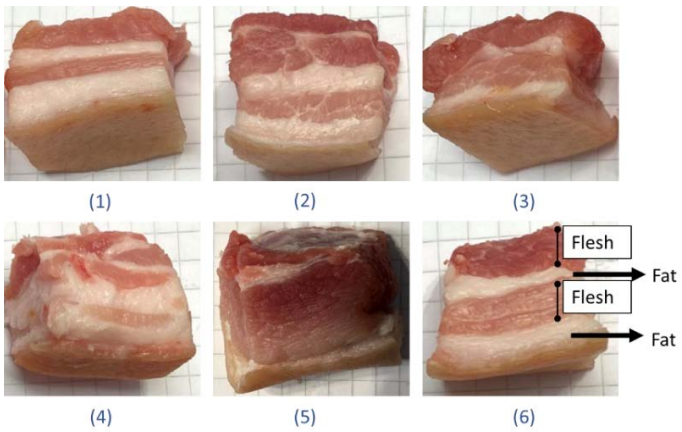

Figure 18. Six individual meat samples

The variations in the power transmitted through the six different samples are presented in Figure 23. It can be clearly seen that the transmitted power through the sample number 5 is significantly lower than the power of the rest of the samples. The dense layer of meat in this sample causes this loss of transmitted power. Although, the other five samples are not completely homogeneous in structure but all of those are comprised of multiple layers of both fat and flesh. The transmitted power through these samples suffers fewer variations from each other mostly due to the thicker fat layers. The average output power of these five samples is 305.92 µW.

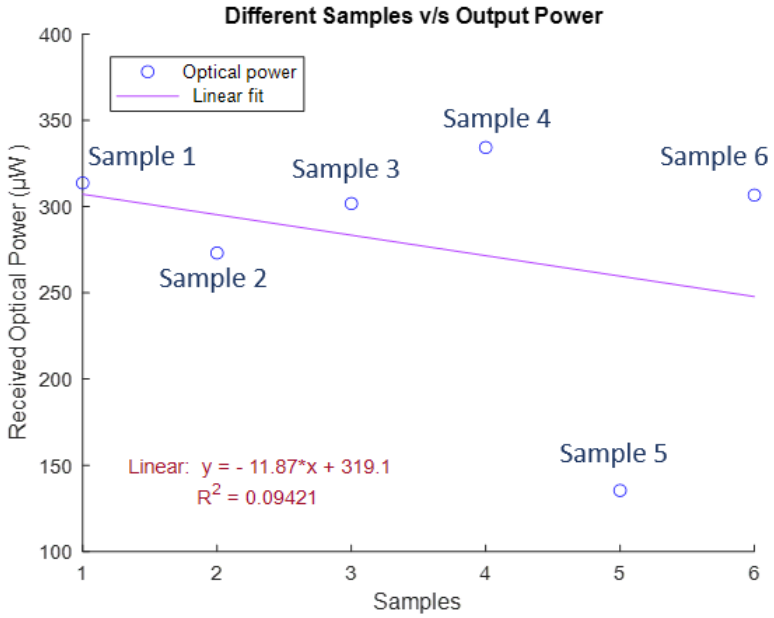

Figure 19. Variation of output power on different samples

5.2.5 Impact of Tissue Orientation

One of the experiments for this work has been conducted using a 2 cm squared solid piece of meat. There is no skin attached to this meat piece. It consists of 0.5 cm of the fat layer and another 1.5 cm layer of flesh. The measurements of this sample have been carried out without the use of a focusing lens for LED. The purpose of this experiment with a meat sample without the skin is to check whether the orientation of tissue structure causes any effect on optical communication through biological tissue. The transmitted power through the tissue sample has been measured for the variation of the LED input current. The first set of measurements was taken with the meat sample placed randomly as an optical medium for communication. At the time of the second set of measurements, the same procedure has been followed with the meat sample in a 180 degrees flipped position. As a result, optical communication was established through a different tissue orientation of the same sample of tissue. Figure 24 illustrates the change in received optical power with respect to varying current levels for both flipped and non-flipped meat samples. A clear difference in transmitted power can be noticed for these two cases. Moreover, the transmitted power through the sample without having the skin appears to be much higher than those of the samples having the skin on.

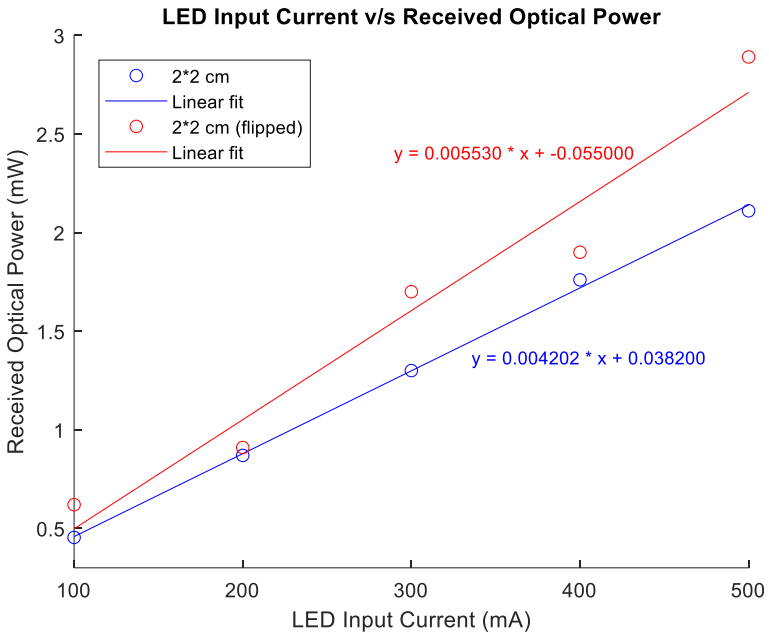

Figure 20. LED input current v/s received optical power

Moreover, the 3 cm thick meat sample has been flipped by 180 degrees to investigate the optical anisotropy of biological tissue. First, the light was applied to the skin surface of the meat sample and the received optical powers at varying input current levels have been measured. Then, the meat sample was flipped so that the flesh surface could face the light rays. The same measurements were taken with this setup. The first setup can be considered as the optical communications from outside to the inside of the body. Similarly, the other setup can be considered as optical communications from inside to the outside of the body. Figure 25 presents the effect of optical anisotropy of the biological tissue on the received optical power. Due to the change in refractive indices for the two measurement setups, a slight difference in receive optical powers can be noticed.

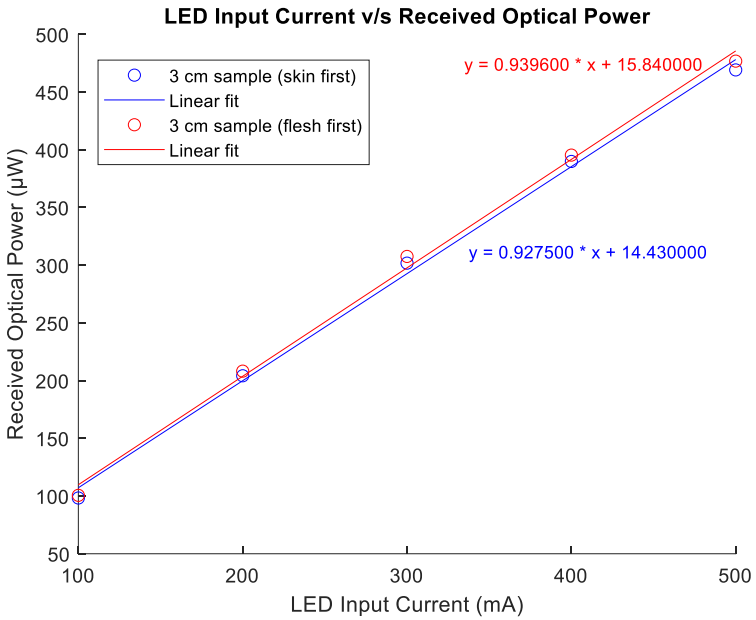

Figure 25. LED input current v/s received optical power

5.2.6 Impact of Sample Thickness

Here, four meat samples having a thickness of 1 cm, 2 cm, 2.5 cm, and 3 cm have been chosen for the experiment. All the samples are taken from the same chunk of belly meat. However, we avoided cutting the same 3 cm sample (used for the previous measurement) down to our required thicknesses. Since the 3 cm meat piece consists of multiple layers of fat and flesh, cutting this piece to 1 cm thick slice would have resulted in a sample with only a fat element. The same procedures have been applied to these four different thick samples to investigate the penetration of light through these. The effect of tissue thickness on the light penetration and received optical power is illustrated in Figure 26. With the increase of tissue thickness, the received optical power through the tissue dropped significantly.

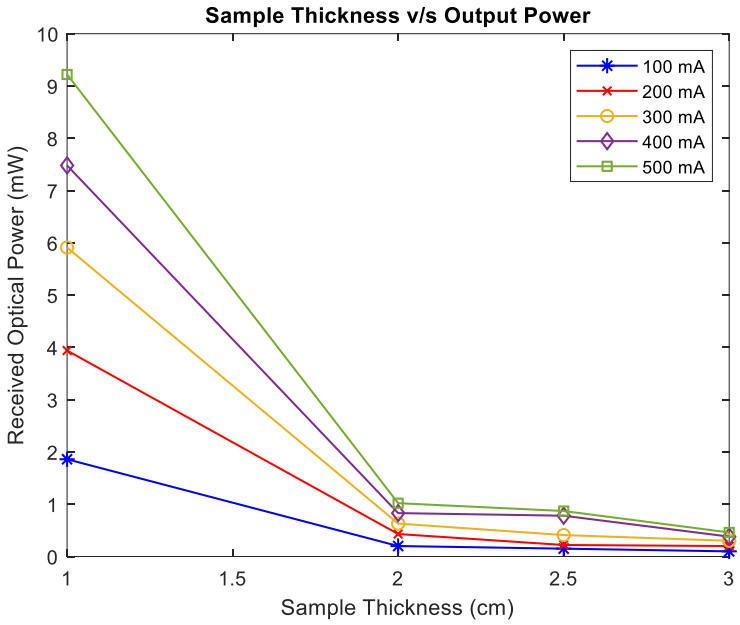

Figure 21. Sample thickness v/s output power

The transmittance rate of these four samples has also been measured and compared. Transmittance is used to determine the total amount of light that usually passes through a particular medium. As expected, the transmittance rate of a 1 cm thick sample was found to be maximum among all the samples. Whereas the 3 cm thick sample had the minimum transmittance rate. The transmittance rate with respect to varying LED input current for 1 cm, 2 cm, 2.5 cm, and 3 cm thick meat samples are presented in Tables 3, 4, 5, and 6 respectively.

Table 3. Transmittance rate for 1 cm thick sample

Thickness (cm)	LED Input Current (mA)	Incident Power (mW/cm^2)	Received Power (mW/cm^2)	Transmittance (%)
1	100	50.94	1.86	3.65
	200	101.11	3.94	3.89
	300	146.26	5.91	4.04
	400	190.53	7.48	4.00
	500	231.38	9.22	3.98

Table 4. Transmittance rate for 2 cm thick sample

Thickness (cm)	LED Input Current (mA)	Incident Power (mW/cm^2)	Received Power (mW/cm^2)	Transmittance (%)
2	100	50.94	0.2	0.39
	200	101.11	0.43	0.43
	300	146.26	0.63	0.43
	400	190.53	0.83	0.44
	500	231.38	1.02	0.44

Table 5. Transmittance rate for 2.5 cm thick sample

Thickness (cm)	LED Input Current (mA)	Incident Power (mW/cm^2)	Received Power (mW/cm^2)	Transmittance (%)
2.5	100	50.94	0.15	0.29
	200	101.11	0.22	0.22
	300	146.26	0.41	0.30
	400	190.53	0.78	0.41
	500	231.38	0.87	0.38

Table 6. Transmittance rate for 3 cm thick sample

Thickness (cm)	LED Input Current (mA)	Incident Power (mW/cm^2)	Received Power (mW/cm^2)	Transmittance (%)
3	100	50.94	0.09	0.19
	200	101.11	0.2	0.20
	300	146.26	0.3	0.21
	400	190.53	0.38	0.20
	500	231.38	0.46	0.19

5.2.7 Measurement Results Using Phantoms

Here, we have conducted experiments to wirelessly transmit data through biological phantoms utilizing NIR light of 810 nm wavelength. We have used five phantoms with scattering coefficients of 1 mm^{-1}, 2 mm^{-1}, 4 mm^{-1}, 6 mm^{-1}, and 10 mm^{-1}. Along with establishing optical communications through all the separate phantoms, we have successfully transmitted the same image file that we have used for pork meat samples before. The experimental setup of optical communication through the phantom mimicking skin is presented in Figure 27.

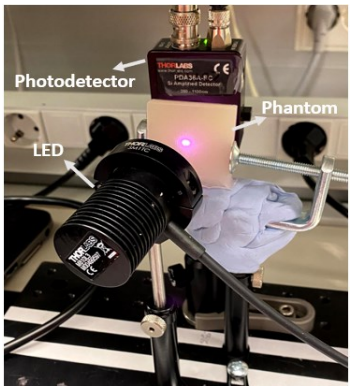

Figure 22. Experimental setup for optical communication through phantom

For these phantoms, during the measurements the input current of LED was set to 300 mA. Table 7 represents the incident power and received power through the six different phantoms.

Table 7. Incident and received power to the phantoms

Scattering Coefficient (mm^{-1})	Incident Power (mW/cm^2)	Received Power (mW/cm^2)
1	146.26	16.45
2	146.26	4.05
4	146.26	3.02
6	146.26	2.94
10	146.26	1.98

Figure 28 shows the received optical power of the phantoms with respect to the scattering coefficients. It can be seen that the maximum received power was obtained for the phantom with a scattering coefficient of 1 mm^{-1}. As the scattering coefficients per mm unit of the phantoms get increased, a significant loss in the transmitted power can be noticed.

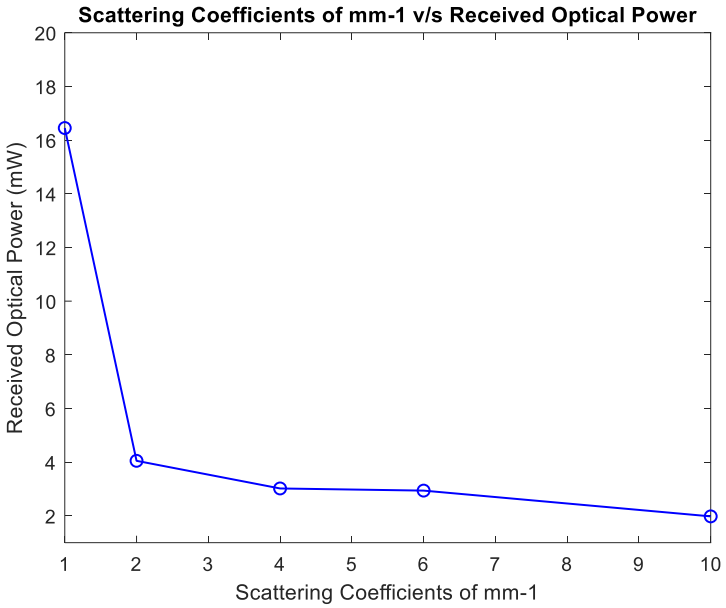

Figure 23. Scattering coefficients of mm^{-1} v/s received optical power

5.3 Characterization of Tissues and Communication Links

The process of light propagation through biological tissues is highly complex. Various parameters such as scattering, absorption, reflectance are extremely important to better understand the concept of light propagation through biological tissues. Here, based on the measurement results from the conducted experiments, we have tried to characterize the communication links, used tissues, and their different parameters.

The manner in which the light rays hit the biological tissue surface holds great importance when the proper optical communication through the tissue is concerned. Here, we have conducted experiments to understand the impact of beam collimation on optical communications. Beam collimation has a significant effect on the penetration of light through an optical medium. The proper usage of the focusing lens is utilized mainly to narrow down the light rays, which is very crucial for successful OCBT. Therefore, good care should be taken for the precise placement of the focusing lens. Ideally, optical communication through tissues with

the help of beam collimation should provide better results compared to the communication without using a collimated beam. However, according to our measurements, for 100 mA input current the transmitted power through 3 cm thick tissue with and without the beam collimation is 52.3 $\mu W/cm^2$ and 98.3 $\mu W/cm^2$, respectively. Due to small size of the meat sample, boundary reflection played a significant role which has caused this lower optical power after using the lens. Moreover, transmitted power through the tissue is inversely proportional to the distance between the surface of the lens and tissue sample. With the increase of this distance, we have noticed a continuous decrease in the output power of the tissue. In order to completely focus all of the light rays on the tissue, the distance between the surface of the lens and tissue needs to be chosen accurately.

The temperature of the tissue sample also has an effect on the behaviour of optical communications through biological tissue. When comparing the transmitted power through a cold and heated version of the same sample, a slight rise in the received power through a heated sample was noticed. Therefore, it can be assumed that light rays tend to penetrate better through heated meat pieces since the heat helps the fat layer of meat to be transparent. Here, we have found the maximum received optical power to be 469.2 $\mu W/cm^2$ and 496.4 $\mu W/cm^2$ for meat at 11 and 37°C, respectively.

The repeatability test is considered to be an essential element during the measurement process. This test helps to determine the variations regarding the measurement data. There are some conditions such as, same experimental procedure, same measurement tools, same parameters, and locations that are required to follow during a repeatability test. One of the major limitations during our measurement process was that we have not determined the uncertainties of the received optical power with respect to a fixed LED input current. However, we have conducted an inter-sample repeatability test to observe the uncertainties. Here, the *p*-value measured during the inter-sample repeatability test is 0.713. This illustrates that the measurement process followed in this work would give an accurate result for various tissue samples.

Experiments conducted by utilizing six individual samples of similar thickness provide valuable information regarding the characteristic of the used tissue. From the experiment, it is seen that the propagation of light is not exactly similar for samples taken from different areas of the pig body. The tissue structure plays a big role in determining how the light will propagate through it. Light propagation through the fat layer seems to be better compared to the propagation of light through dense muscle tissue. Tissue samples with more fat layers experience less amount of transmitted power loss.

We have seen significant variations in the transmitted power through tissue samples having different thicknesses. The received optical power from a tissue sample with relatively small thickness has been found to be higher, as expected. Also, for the samples with less thickness need less input current for optical communication through them. This can be viewed as a key characteristic while wireless optical communication through biological tissue is concerned. Some implantable medical devices are located very close to the skin. One such device is pacemaker which is typically located just under the collar bone and several millimetres away from the skin surface. This key characteristic could be very beneficial for establishing optical wireless communication with medical implants. Additionally, the transmittance rate can be regarded as another vital parameter for realizing the propagation of light through biological tissues.

We have noticed a difference in the received optical power between different propagation directions due to the anisotropic light propagation in biological tissues. So, it can be said that the effect of optical anisotropy is also visible from the wireless communications standpoint.

Transmission ranges of up to 3 cm have been demonstrated in this work. This is a quite significant range, allowing communications in principle to more deeply located devices. The optical link was not matched perfectly to the optical channel. It is believed that higher data throughput can be obtained once the optical channel of biological tissues is precisely modelled and a received matched to it can be designed.

6 DISCUSSION AND CONCLUSION

This thesis work investigates the potentiality of utilizing light rays for optical communication through the biological tissues. An experimental testbed comprised of mostly commercially available functionalities and components were used to carry out the measurements. An optical transmitter, suitable communication medium, an optical receiver are the fundamental components of our testbed. Biological phantoms and pork meat samples have been employed as optical media. The phantoms and meat samples were illuminated with the help of a near-infrared LED at a wavelength of 810 nm. Since the NIR light penetrates deeply through the biological tissue, we have chosen this to be the light source for our experiments.

Here, we have demonstrated a successful optical transmission of information through a 3 cm thick pork meat sample. The optical communication was successful using the biological phantoms mimicking human skin as well. The amount of optical power applied to the meat sample at the time of communication was much lower than the safety limit. We have performed testing on both cold and heated samples and optical communication has been successful for both the cases. However, the change of tissue temperature has caused a variation in the optical received power of the tissue samples. The optical received power of the heated tissue sample was appeared to be higher compared to that of the cold tissue sample. Moreover, the positioning of the focusing lens used for beam collimation holds the utmost significance on the transmittance rate. Besides, the measure of transmitted power through the tissue relies on the components of the tissue structure. Heterogeneity of the elemental composition of the tissue that is anisotropy has a substantial influence on the propagation of light through tissue. These results suggest that the optical channel is not reciprocal, and special care should be taken when designing links to and from devices inside the human body. We have extended our measurements by alternating the surface of tissue in which the NIR light was applied to better understand the optical properties of biological tissue. A considerable amount of variation in the received optical power has been noticed because of this change in orientation of the tissue sample. Not only light at wavelengths in the NIR zone (650nm-950nm) typically possesses the highest penetration depth in tissue, also it gets less affected by the scattering and absorption properties of the tissue. In spite of these characteristics of light, still, with the increase in the thickness of the meat sample, we have seen a significant loss in terms of transmittance rate. The data rate during the OCBT has been found to be in the order of tens Kbps which is relatively low. However, this low data rate can be very useful in some applications concerning implantable medical devices. Using more sophisticated modulation schemes as well as multiple light beams could be solutions to increase the achievable data rate. Also, once the optical channels are fully understood and modelled, as communication systems matched to the channel can be designed.

Plenty of potential advantages are associated with the concept of optical communication through biological tissue. The measurement results of our experiment indicate a number of possible future applications of optical wireless communications, particularly in healthcare applications. Optical wireless communication can well be utilized in various implantable medical devices. Certain drawbacks regarding conventional RF communication like interference, safety, energy, security, and privacy can be avoided as well as resolved with the use of optical communication. Communication using light source does not experience interference like typical RF communication and this can be beneficial in various environments. Radio exposure during the RF communication could hamper the properties of biological tissues and this perhaps can be overcome with the use of light. Optical communication needs quite less power to be operated and is considered as a great advantage. Mostly LOS configuration is

required as optical communication is concerned. This characteristic has the ability to protect the medical implants from any kind of unauthorized access thus wellness and safety of the patients is ensured. The light-based communication system is a highly complementary approach to radio-based communication. A highly flexible hybrid optical-radio wireless network having several potential application cases has also been exploited in this thesis work. With all these advantages, we can say that optical wireless communications could be regarded as a more favourable choice for future medical technology. A variety of functions related to medical ICT particularly, treatment and diagnostics can be conducted using this significantly reliable and secure optical wireless communications. Thus, the results obtained from this work could make an important contribution to the advancement of 6G technology. Novel applications related to the use of optical communications in biological tissues include communication with smart pills, the concept of internet of the human body (IoHB), brain-machine communications, and others.

Some hardware limitations associated with the experimental testbed results in obtaining relatively low optical power and data transmission rate. Although, these measurement results are quite satisfactory but more extensive measurements will be carried out in the future to better understand the feasibility of using light for communicating through biological tissues. With the use of more advanced hardware and different modulation schemes, we expect an increase in the data transmission rate and communication range. Moreover, pulsed communications (e.g., high power over short periods) which provide low duty cycles can also help to increase communication range. In addition to the proper modifications of the testbed, the future work will be based on addressing and overcoming the challenges related to the OCBT using different forms of biological tissues.

7 REFERENCES

[1] Cisco, “Cisco Annual Internet Report (2018–2023),” *Cisco*, pp. 1–41, 2020.

[2] M. Katz, M. Matinmikko-blue, and M. Latva-aho, “6Genesis Flagship Program : Building the Bridges towards 6G-enabled Wireless Smart Society and Ecosystem.”

[3] A. P. Ed, “6G White Paper on Validation and Trials for Verticals towards 2030 ’ s,” 2020.

[4] I. Ahmed, A. Bykov, A. Popov, I. Meglinski, and M. Katz, “Optical Wireless Data Transfer Through Biotissues: Practical Evidence and Initial Results,” *Lect. Notes Inst. Comput. Sci. Soc. Telecommun. Eng. LNICST*, vol. 297 LNICST, pp. 191–205, 2019, doi: 10.1007/978-3-030-34833-5_16.

[5] C. Camara, P. Peris-Lopez, and J. E. Tapiador, “Security And Privacy Issues In Implantable Medical Devices: A Comprehensive Survey,” *J. Biomed. Inform.*, vol. 55, pp. 272–289, 2015, doi: 10.1016/j.jbi.2015.04.007.

[6] J. C. Zwinkels and C. Canada, “Encyclopedia of Color Science and Technology,” *Encycl. Color Sci. Technol.*, no. January 2015, 2019, doi: 10.1007/978-3-642-27851-8.

[7] T. Pulli, T. Dönsberg, T. Poikonen, F. Manoocheri, P. Kärhä, and E. Ikonen, “Advantages of White LED Lamps and New Detector Technology in Photometry,” *Light Sci. Appl.*, vol. 4, no. June, pp. 1–7, 2015, doi: 10.1038/lsa.2015.105.

[8] C. Singh, J. John, Y. N. Singh, and K. K. Tripathi, “A Review of Indoor Optical Wireless Systems,” *IETE Tech. Rev. (Institution Electron. Telecommun. Eng. India)*, vol. 19, no. 1–2, pp. 3–17, 2002, doi: 10.1080/02564602.2002.11417006.

[9] R. A. Rajan Sagotra, “Visible Light Communication,” *Int. J. Comput. Trends Technol. - Vol. –April 2013*, vol. 4, no. April, 2013, doi: 10.1017/CBO9781107447981.

[10] J. L. S. J. M. Avella, T. Souza, “A Comparative Analysis between Fluorescent and LED Illumination for Improve Energy Efficiency at IPBEN Building,” *Xi Latin-American Congr. Electr. Gener. Transm.*, no. November, p. [1] J. Mario and A. Ruiz, “A Comparative Analysis, 2015.

[11] A. Sevincer, A. Bhattarai, M. Bilgi, M. Yuksel, and N. Pala, “Lightnets: Smart Lighting and Mobile Optical Wireless Networks - A Survey,” *IEEE Commun. Surv. Tutorials*, vol. 15, no. 4, pp. 1620–1641, 2013, doi: 10.1109/SURV.2013.032713.00150.

[12] A. R. Ndjiongue, H. C. Ferreira, and T. M. N. Ngatched, “Visible Light Communications (VLC) Technology,” *Wiley Encycl. Electr. Electron. Eng.*, no. Vlc, pp. 1–15, 2015, doi: 10.1002/047134608x.w8267.

[13] P. H. Pathak, X. Feng, P. Hu, and P. Mohapatra, “Visible Light Communication, Networking, and Sensing: A Survey, Potential and Challenges,” *IEEE Commun. Surv. Tutorials*, vol. 17, no. 4, pp. 2047–2077, 2015, doi: 10.1109/COMST.2015.2476474.

[14] J. R. B. Kwonhyung Lee, Hyuncheol Park, "Indoor Channel Characteristics for Visible Light Communications," *IEEE Commun. Lett. VOL. 15, NO. 2, Febr. 2011*, vol. 53, no. 10, p. 106101, 2014, doi: 10.1117/1.oe.53.10.106101.

[15] J. M. Kahn and J. R. Barry, "Wireless Infrared Communications," *Proc. IEEE*, vol. 85, no. 2, pp. 265–298, 1994.

[16] Chung Ghiu Lee, "Visible Light Communication," *Visible Light Commun.*, no. March, pp. 1–210, 2015, doi: 10.1017/CBO9781107447981.

[17] T. Cevik and S. Yilmaz, "An Overview of Visible Light Communication Systems," *Int. J. Comput. Networks Commun.*, vol. 7, no. 6, pp. 139–150, 2015, doi: 10.5121/ijcnc.2015.7610.

[18] G. Blinowski, "Security Issues in Visible Light Communication Systems," *IFAC-PapersOnLine*, vol. 28, no. 4, pp. 234–239, 2015, doi: 10.1016/j.ifacol.2015.07.039.

[19] D. C. O. Brien, L. Zengl, H. L. Grahame, J. Walewski, and S. Randel, "Visible Light Communications: Challenges and Possibilities," pp. 1–5, 2008.

[20] M. Saadi, L. Wattisuttikulkij, Y. Zhao, and P. Sangwongngam, "Visible Light Communication: Opportunities, Challenges and Channel Models," *Int. J. Electron. Informatics*, vol. 2, no. 1, pp. 1–11, 2013.

[21] L. E. M. Matheus, A. B. Vieira, L. F. M. Vieira, M. A. M. Vieira, and O. Gnawali, "Visible Light Communication: Concepts, Applications and Challenges," *IEEE Commun. Surv. Tutorials*, vol. PP, no. c, p. 1, 2019, doi: 10.1109/COMST.2019.2913348.

[22] C. W. Chow, C. H. Yeh, Y. F. Liu, and Y. Liu, "Improved Modulation Speed of LED Visible Light Communication System Integrated to Main Electricity Network," *Electron. Lett.*, vol. 47, no. 15, pp. 867–868, 2011, doi: 10.1049/el.2011.0422.

[23] K. P. Pujapanda, "Lifi Integrated to Power-Lines for Smart Illumination Cum Communication," *Proc. - 2013 Int. Conf. Commun. Syst. Netw. Technol. CSNT 2013*, pp. 875–878, 2013, doi: 10.1109/CSNT.2013.189.

[24] J. Cho, J. H. Park, J. K. Kim, and E. F. Schubert, "White Light-Emitting Diodes: History, Progress, and Future," *Laser Photonics Rev.*, vol. 11, no. 2, 2017, doi: 10.1002/lpor.201600147.

[25] D. Karunatilaka, F. Zafar, V. Kalavally, and R. Parthiban, "LED Based Indoor Visible Light Communications: State of The Art," *IEEE Commun. Surv. Tutorials*, vol. 17, no. 3, pp. 1649–1678, 2015, doi: 10.1109/COMST.2015.2417576.

[26] J. Lian, Z. Vatansever, M. Noshad, and M. Brandt-Pearce, "Indoor Visible Light Communications, Networking, and Applications," *J. Phys. Photonics*, vol. 1, no. 1, p. 012001, 2019, doi: 10.1088/2515-7647/aaf74a.

[27] S. Viola, M. S. Islim, S. Watson, S. Videv, H. Haas, and A. E. Kelly, “15 Gb/s OFDM-Based VLC Using Direct Modulation of 450 Gan Laser Diode,” no. October 2017, p. 17, 2017, doi: 10.1117/12.2292004.

[28] R. Ji, S. Wang, Q. Liu, and W. Lu, “High-Speed Visible Light Communications: Enabling Technologies and State of the Art,” *Appl. Sci.*, vol. 8, no. 4, 2018, doi: 10.3390/app8040589.

[29] N. G. Hrushit Parikh, Jimesh Chokshi, “Wirelessly Transmitting a Grayscale Image Using,” *Int. J. Comput. Appl. (0975 –8887) Vol. 58–No.14, Novemb. 2012*, vol. 58, no. 14, pp. 0–5, 2012.

[30] H. Ma, L. Lampe, and S. Hranilovic, “Integration of Indoor Visible Light and Power Line Communication Systems, ” BT - IEEE International Symposium On Power Line Communications And ITS Applications,” pp. 291–296, 2013.

[31] S. Zhao, J. Xu, and O. Trescases, “A Dimmable LED Driver for Visible Light Communication (VLC) Based on LLC Resonant DC-DC Converter Operating in Burst Mode,” *Conf. Proc. - IEEE Appl. Power Electron. Conf. Expo. - APEC*, no. Vlc, pp. 2144–2150, 2013, doi: 10.1109/APEC.2013.6520592.

[32] C. Rohner, S. Raza, D. Puccinelli, and T. Voigt, “Security in Visible Light Communication: Novel Challenges and Opportunities,” *Sensors & Transducers*, vol. 192, no. 9, pp. 9–15, 2015.

[33] M. Biagi, T. Borogovac, and T. D. C. Little, “Adaptive Receiver for Indoor Visible Light Communications,” *J. Light. Technol.*, vol. 31, no. 23, pp. 3676–3686, 2013, doi: 10.1109/JLT.2013.2287051.

[34] T. Borogovac, M. Rahaim, and J. B. Carruthers, “Spotlighting for Visible Light Communications and Illumination,” *2010 IEEE Globecom Work. GC’10*, pp. 1077–1081, 2010, doi: 10.1109/GLOCOMW.2010.5700100.

[35] A. N. Sarkar Anurag, Shalabh Agarwal, “Li-Fi Technology : Data Transmission through Visible Light,” *Int. J. Adv. Res. Comput. Sci. Manag. Stud.*, vol. 3, no. 6, pp. 1–12, 2015.

[36] S. Singh, G. Kakamanshadi, and S. Gupta, “Visible Light Communication-an Emerging Wireless Communication Technology,” in *2015 2nd International Conference on Recent Advances in Engineering & Computational Sciences (RAECS)*, 2015, pp. 1–3, doi: 10.1109/RAECS.2015.7453409.

[37] H. Elgala, R. Mesleh, H. Haas, and B. Pricope, “OFDM Visible Light Wireless Communication Based on White Leds,” *IEEE Veh. Technol. Conf.*, pp. 2185–2189, 2007, doi: 10.1109/VETECS.2007.451.

[38] C. Liu, B. Sadeghi, and E. W. Knightly, “Enabling Vehicular Visible Light Communication (V2LC) Networks,” *Proc. Annu. Int. Conf. Mob. Comput. Networking, MOBICOM*, no. September 2011, pp. 41–50, 2011, doi: 10.1145/2030698.2030705.

[39] G. Blinowski, “Security of Visible Light Communication Systems—A Survey,” *Phys. Commun.*, vol. 34, pp. 246–260, 2019, doi: 10.1016/j.phycom.2019.04.003.

[40] T. Yamazato, I. Takai, H. Okada, T. Fujii, T. Yendo, and S. Arai, “Image-Sensor-Based Visible Light Communication for Automotive Application,” no. July, pp. 88–97, 2014.

[41] N. Farr, N. Farr, A. Bowen, J. Ware, and C. Pontbriand, “An Integrated , Underwater Optical / Acoustic Communications System an Integrated , Underwater Optical / Acoustic Communications System,” *IEEE Xplore*, no. June, 2010, doi: 10.1016/j.ejmech.2015.03.019.

[42] M. Z. and K. N. Carlos Medina, “Led Based Visible Light Communication: Technology, Applications and Challenges – A Survey,” vol. 24, no. April, pp. 54–60, 2015.

[43] S. Haruyama, “Advances in Visible Light Communication Technologies,” *Eur. Conf. Opt. Commun. ECOC*, pp. 5–7, 2012.

[44] A. Jovicic, J. Li, and T. Richardson, “Visible Light Communication: Opportunities, Challenges and the Path to Market,” *IEEE Commun. Mag.*, vol. 51, no. 12, pp. 26–32, 2013, doi: 10.1109/MCOM.2013.6685754.

[45] and S.-K. H. Hyun-Seung Kim, Deok-Rae Kim, Se-Hoon Yang, Yong-Hwan Son, “An Indoor Visible Light Communication Positioning System Using a RF Carrier Allocation Technique,” *J. Light. Technol. VOL. 31, NO. 1, JANUARY 1, 2013*, vol. 31, no. 1, pp. 25–29, 2013, doi: 10.1109/IWOW.2013.6777770.

[46] J. E. Ferguson and A. D. Redish, “Wireless Communication with Implanted Medical Devices Using the Conductive Properties of the Body,” *Expert Rev. Med. Devices*, vol. 8, no. 4, pp. 427–433, 2011, doi: 10.1586/erd.11.16.

[47] M. S. Saud and M. Katz, “Implementation of a Hybrid Optical-RF Wireless Network With Fast Network Handover,” *Eur. Wirel. 2017 - 23rd Eur. Wirel. Conf.*, no. May, 2017.

[48] M. S. Saud, H. Chowdhury, and M. Katz, “Heterogeneous Software-Defined Networks: Implementation of a Hybrid Radio-Optical Wireless Network,” *IEEE Wirel. Commun. Netw. Conf. WCNC*, 2017, doi: 10.1109/WCNC.2017.7925873.

[49] I. Ahmed, T. Kumpuniemi, and M. Katz, “A Hybrid Optical-Radio Wireless Network Concept for the Hospital of the Future,” pp. 1–13.

[50] M. S. Saud, I. Ahmed, T. Kumpuniemi, and M. Katz, “Reconfigurable Optical-Radio Wireless Networks: Meeting the Most Stringent Requirements of Future Communication Systems,” *Trans. Emerg. Telecommun. Technol.*, vol. 30, no. 2, pp. 1–15, 2019, doi: 10.1002/ett.3562.

[51] J. G. Betts *et al.*, Anatomy & Physiology Senior Contributing Authors. 2013.

[52] “Dense Connective Tissue.” [Online]. Available: https://bit.ly/3eawsuo.

[53] S. L. Jacques, “Optical Properties of Biological Tissues: A Review,” *Phys. Med. Biol.*, vol. 58, no. 11, 2013, doi: 10.1088/0031-9155/58/11/R37.

[54] D.-H. Kim, “Fundamentals of Propagation of Light in Tissue,” *Theory Appl. Heat Transf. Humans*, pp. 153–166, 2018, doi: 10.1002/9781119127420.ch9.

[55] A. Kim and B. C. Wilson, “Measurement of *Ex Vivo* and *In Vivo* Tissue Optical Properties : Methods and Theories”. 2011.

[56] D. D. Nolte, “Optical Interferometry for Biology and Medicine”. 2012.

[57] A. J. Welch and M. J. C. Van Gemert, “Optical-Thermal Response of Laser-Irradiated Tissue,” *Opt. Response Laser-Irradiated Tissue*, pp. 1–958, 2011, doi: 10.1007/978-90-481-8831-4.

[58] B. Castellani *et al.*, “Comparative Analysis of Monitoring Devices for Particulate Content in Exhaust Gases,” *Sustain.*, vol. 6, no. 7, pp. 4287–4307, 2014, doi: 10.3390/su6074287.

[59] A. Doronin and I. Meglinski, “Online Object Oriented Monte Carlo Computational Tool for the Needs of Biomedical Optics,” *Biomed. Opt. Express*, vol. 2, no. 9, p. 2461, 2011, doi: 10.1364/boe.2.002461.

[60] S. A. Prahl, “A Monte Carlo Model of Light Propagation in Tissue,” *Dosim. Laser Radiat. Med. Biol.*, vol. 10305, no. June, p. 1030509, 1989, doi: 10.1117/12.2283590.

[61] V. Periyasamy and M. Pramanik, “Advances in Monte Carlo Simulation for Light Propagation in Tissue,” *IEEE Rev. Biomed. Eng.*, vol. 10, pp. 122–135, 2017, doi: 10.1109/RBME.2017.2739801.

[62] L. Wang, S. L. Jacques, and L. Zheng, “MCML-Monte Carlo Modeling of Light Transport in Multi-Layered Tissues,” *Comput. Methods Programs Biomed.*, vol. 47, no. 2, pp. 131–146, 1995, doi: 10.1016/0169-2607(95)01640-F.

[63] A. Doronin and I. Meglinski, “Peer-To-Peer Monte Carlo Simulation of Photon Migration in Topical Applications of Biomedical Optics,” no. May 2014, 2012, doi: 10.1117/1.JBO.17.9.090504.

[64] “Cloud Monte Carlo for Light Transport in Turbid Scattering Medium.” [Online]. Available: http://biophotonics.fi/.

[65] M. S. Wróbel, A. P. Popov, A. V. Bykov, V. V. Tuchin, and M. Jędrzejewska-Szczerska, “Nanoparticle-Free Tissue-Mimicking Phantoms with Intrinsic Scattering,” *Biomed. Opt. Express*, vol. 7, no. 6, p. 2088, 2016, doi: 10.1364/boe.7.002088.

[66] M. S. Wróbel, A. P. Popov, A. V. Bykov, M. Kinnunen, M. Jedrzejewska-Szczerska, and V. V. Tuchin, “Measurements of Fundamental Properties of Homogeneous Tissue Phantoms,” *J. Biomed. Opt.*, vol. 20, no. 4, p. 045004, 2015, doi: 10.1117/1.jbo.20.4.045004.

[67] A. V. Bykov, A. P. Popov, A. V. Priezzhev, and R. Myllylä, "Multilayer Tissue Phantoms with Embedded Capillary System for OCT and DOCT Imaging," *Opt. InfoBase Conf. Pap.*, no. July 2014, 2011, doi: 10.1117/12.889923.

[68] B. W. Pogue and M. S. Patterson, "Review of Tissue Simulating Phantoms for Optical Spectroscopy , Imaging and Dosimetry," vol. 11, no. August 2006, pp. 1–16, 2020, doi: 10.1117/1.2335429.

[69] M. S. Wr, A. P. Popov, A. V Bykov, and M. Kinnunen, "Multi-Layered Tissue Head Phantoms for Noninvasive Optical Diagnostics," vol. 8, no. 3, pp. 1–10, 2015, doi: 10.1142/S1793545815410059.

[70] A. V Bykov, A. Popov, M. Kinnunen, and A. Priezzhev, "Skin Phantoms with Realistic Vessel Structure for OCT Measurements," no. June, 2010, doi: 10.1117/12.872000.

[71] R. Srinivasan, D. Kumar, and M. Singh, "Optical Tissue-Equivalent Phantoms for Medical Imaging," no. March, 2016.

[72] M. Szczerska, S. Galla, and M. Sawczak, "Use of Optical Skin Phantoms for Preclinical Evaluation of Laser Efficiency for Skin Lesion Therapy," no. August, 2015, doi: 10.1117/1.JBO.20.8.085003.

[73] L. A. Sordillo, Y. Pu, and R. Alfano, "Deep Optical Imaging of Tissue Using the Second and Third Near-Infrared Spectral Windows," no. May, pp. 3–10, 2014, doi: 10.1117/1.JBO.19.5.056004.

[74] F. B. Serkin and N. A. Vazhenin, "USRP Platform for Communication Systems Research," *Int. Conf. Transparent Opt. Networks*, no. Ddc, pp. 1–4, 2013, doi: 10.1109/ICTON.2013.6602738.

[75] "USRP Software Defined Radio Device." [Online]. Available: https://www.ni.com/fi-fi/shop/select/usrp-software-defined-radio-device?modelId=125048.

[76] P. Kamsula, "Design and Implementation of a Bi-directional Visible Light Communication Testbed," University of Oulu, 2015.

[77] H. Chowdhury, "Data Download on the Move in Visible Light Communications : Design and Analysis," 2016.

[78] "Thorlabs Mounted LEDs." [Online]. Available: https://bit.ly/2N9uI8Y.

[79] "Thorlabs DC2200 LED Driver." [Online]. Available: https://bit.ly/2VaFGj5.

[80] "SM2F32-B - Adjustable Collimation Adapter." [Online]. Available: https://bit.ly/2UV9mR0.

[81] T. Turletti, "GMSK in a nutshell," no. April, 2013.

[82] J. D. Gibson, “The Mobile Communications Handbook”.

[83] “Thorlabs APD120A/M - Si Avalanche Photodetector, 400 - 1000 nm, M4 Taps.” [Online]. Available: https://bit.ly/2UTIDUS.

[84] “American National Standard for Safe Use of Lasers.” [Online]. Available: https://assets.lia.org/s3fs-public/pdf/ansi-standards/samples/ANSI Z136.1_sample.pdf.

[85] S. Plog, L. Mundhenk, M. K. Bothe, N. Klymiuk, and A. D. Gruber, “Tissue and Cellular Expression Patterns of Porcine CFTR : Similarities to and Differences From Human CFTR The Journal of Histochemistry & Cytochemistry,” vol. 58, no. 9, pp. 785–797, 2010, doi: 10.1369/jhc.2010.955377.

[86] “Tissue-mimicking Phantoms.” [Online]. Available: https://bit.ly/2UTZ5Vk.